JAERI - M
88-109

ESTIMATION OF TOROIDAL FIELD COIL STRESSES FROM MAGNETIC LOADS IN FER AND NET USING ANALYTIC METHODS AND IMPROVED COMPUTER SUBROUTINE FOR TFC STRESS ESTIMATION IN TRESCODE

June 1988

Bernard W. RIEMER*, Nobuharu MIKI and Takashi HASHIZUME**

日 本 原 子 力 研 究 所
Japan Atomic Energy Research Institute

JAERI-Mレポートは，日本原子力研究所が不定期に公刊している研究報告書です。
入手の問合わせは，日本原子力研究所技術情報部情報資料課（〒319-11茨城県那珂郡東海村）あて，お申しこしください。なお，このほかに財団法人原子力弘済会資料センター（〒319-11 茨城県那珂郡東海村日本原子力研究所内）で複写による実費頒布をおこなっております。

JAERI-M reports are issued irregularly.
Inquiries about availability of the reports should be addressed to Information Division, Department of Technical Information, Japan Atomic Energy Research Institute, Tokai-mura, Naka-gun, Ibaraki-ken 319-11, Japan.

編集兼発行　日本原子力研究所
印　　刷　㈱原子力資料サービス

Estimation of Toroidal Field Coil Stresses from Magnetic Loads in FER and NET Using Analytic Methods and Improved Computer Subroutine for TFC Stress Estimation in TRESCODE

Bernard W. RIEMER*, Nobuharu MIKI and Takashi HASHIZUME**

Department of Large Tokamak Research
Naka Fusion Research Establishment
Japan Atomic Energy Research Institute
Naka-machi, Naka-gun, Ibaraki-ken

(Received May 19, 1988)

This report describes the comparison of TF coil stresses in NET and FER. The analyses focus on the straight part of the inner legs, since it is this part of the coil which most directly influences the radial build of the machine. NET's TF coils are wedged together and the centering force on each of the coils is reacted by toroidal compression of the inner legs. The forces that act out of the plane of each coil are reacted by friction between adjacent inner legs such that the set of legs behave much like a cylinder under torsion. In contrast, the FER device employs a bucking cylinder to react the centering load, which incurs a penalty in radial thickness, and the out of plane forces are reacted by the use of shear keys between adjacent inner legs.

Analytic techniques or "hand methods" have been used to estimate and compare the strains and stresses at the inner leg mid-plane section resulting from both in-plane and out-of-plane magnetic forces. Such techniques forced a more thorough understanding of the structural behavior of the coils. The amount of effort in analyizing the NET

---

* Oak Ridge National Laboratory
** Kawasaki Heavy Industries, Ltd.

coil is greater than for FER as the reaction of centering load in its wedged design is more complex, and because it was found that friction plays a very important part in determining the coil stresses. The FER coil is simpler in this regard, and a "hand estimation" of its coil stresses was straightfoward.

In this report, the program written to perform these analyses is also described. It was desired to provide new capabilities to the original TF stress subroutine in TRESCODE and to review and improve it where possible. This has been accomplished, and subroutines are now available for use in JAERI's system code, TRESCODE. It is hoped that the inner leg radial thickness can be better optimized by using the program.

Keywords: Fusion Experimental Reactor (FER), Next European Torus (NET), Toroidal Field Coil, Coil Inner Leg, Wedging Support, Bucking Cylinder Support, In-plane Force, Out-of-plane Force, Coil Stress, Analytic Technique

JAERI－M 88－109

FERとNETのトロイダル磁場コイル内側脚に関する解析的手法による応力評価および計算コードの改良

日本原子力研究所那珂研究所臨界プラズマ研究部
Bernard W・RIEMER*・三木 信晴・橋爪 隆**

（1988年5月19日受理）

本報告書では，NETとFERにおけるTFコイル応力の比較を述べる。装置のラジアルビルドに大きな影響を与えるのは，TFコイル内側脚の直線部であるため，その部分に焦点を当てて検討した。NETのTFコイルはウェッジ支持方式であり，向心力はTFコイル内側脚のトーラス方向の圧縮応力で支持される。面外力は内側脚のコイル間での摩擦によって支持される。一方，FERのTFコイルは中心支柱支持方式であり，向心力は中心支柱で支持される。ウェッジ支持方式に比べて，内側脚全体の半径方向厚さが大きくなる欠点がある。面外力は，内側脚のコイル間に設けたシェアキーで支持される。

面内力および面外力によって内側脚に生じる歪と応力は，解析的な方法で評価された。そのため，コイルの変形，応力の生じ方を考え，より深く理解する必要があった。ウェッジ支持では応力の生じ方がより複雑であること，および巻線とコイル容器間の摩擦力の影響があることのため，NETコイルの応力評価に時間を要した。FERコイルでは電磁力の伝わり方がシンプルであり，比較的簡単に応力評価ができた。

本報告書では，解析のために作成したプログラムについても述べる。開発された解析の手法は，システムコードTRESCODEのサブルーチンの改良に用いられた。

那珂研究所：〒311－01 茨城県那珂郡那珂町大字向山801－1
＊オークリッジ研究所
＊＊川崎重工業（株）

Contents

目　　次

Introduction

In tokamak reactor design perhaps the two most developed concepts for next step devices are the European community's Next European Torus (NET) and Japan's Fusion Experimental Reactor (FER). Despite the fact that they have similar missions, their design approaches differ significantly in a number of areas. This work compares one such area, the Toroidal Field coils; in particular, the stresses developed in the inner legs of the coils are compared in order to see how efficiently the radial thickness of the inner legs is used to support the magnetic loads generated during normal operation of the device. NET's TF coils are wedged together and the centering force on each of the coils is reacted by toroidal compression of the inner legs. The forces that act out of the plane of each coil are reacted by friction between adjacent inner legs such that the set of legs behave much like a cylinder under torsion. In contrast, the FER device employs a bucking cylinder to react the centering load, which incurs a penalty in radial thickness, and the out of plane forces are reacted by the use of shear keys between adjacent inner legs.

Early in the course of this work it was decided to limit the methods used to analytical techniques, and to forego use of finite element programs. This was done for several reasons, not the least of which was that the scale of the task would be increased because of the tremendous detail involved in FEA. Such work is best left to the respective design teams. Since this work was a learning experience, it was preferred to use analytic techniques, or "hand methods", in order to force a more thorough understanding of the structural behavior of the coils. It was believed that because it would be necessary to thoroughly think through each step of modelling assumptions and simplifications, more sense could then be made of the results of highly (at times, overwhelmingly) detailed FEA, and in the future a broader base would be made for confirming such FEA solutions.

It was also desired to be able to program the methodology used in a way suitable for use in a systems code, thus providing a means of more accurately estimating TF stresses. This has been accomplished, and subroutines are now available for use in JAERI's system code, TRESCODE. It is hoped that the inner leg radial thickness can be better optimized by using the program.

This report is in two parts. The first contains description of the analysis methods used for NET and FER, and a comparison of the results obtained. The amount of effort in analyizing the NET coil is greater than for FER as the reaction of centering load in its wedged design is more complex, and because it was found that friction plays a very important part in determining the coil stresses. The FER coil is simpler in this regard, and a "hand estimation" of its coil stresses was straightfoward. The second part of this report addresses the program written to perform these analyses, and it is complemented by an appendix of notes for future users and programers of the subroutine.

I. Analyses Methods

1. Objectives and Scope

The analyses focus on the straight part of the inner legs, since it is this part of the coil which most directly influences the radial build of the machine. Some analysis was performed for the whole NET coil for reacting out-of-plane loads, but as will be seen later in section 3.1, its usefulness was judged to be limited. The in-plane stresses are estimated first, and later torsional shear stresses from out-of-plane loads are estimated. These shear stresses are needed to see how much of an increase there will be in the Von-Mises stress, to find the stress in the shear keys of FER, and in the case of NET, to see if they exceed the capacity of friction between adjacent coils. They are also compared to a cyclic stress allowable.

In this report nomemclature used by the FER team is adopted. The term "outer ring" means the part of the coil case on the side of the winding pack farthest from the plasma. The term "inner ring" means the part of the coil case on the side of the winding pack closest to the plasma. The side plates are the case parts next to the remaining sides of the winding pack. The "inner leg" of the coil is the straight part closest to the machine centerline.

2. Stresses from In-plane Loads

The first step is to estimate the stresses resulting from in-plane loads for both machines. The NET double null machine and the 1986 Advanced Option C FER are the selected options. Some parameters are shown in Table 1, and Figs. 1 & 2 show each machines' TF coil configurations. A sectional view of the inner legs at mid-plane can be seen in Fig. 3. NET has a significant advantage in radial thickness and in overall current density by not having a bucking cylinder.

Constant tension behavior for both machines is assumed. In both cases the coil shapes deviate from true constant tension shape, but their designs are intended to produce constant tension behavior by appropriately adjusting the stiffness of the structure around the coil perimeter. The achievement of this for both is considered apriori for this study.

I. Analyses Methods

1. Objectives and Scope

The analyses focus on the straight part of the inner legs, since it is this part of the coil which most directly influences the radial build of the machine. Some analysis was performed for the whole NET coil for reacting out-of-plane loads, but as will be seen later in section 3.1, its usefulness was judged to be limited. The in-plane stresses are estimated first, and later torsional shear stresses from out-of-plane loads are estimated. These shear stresses are needed to see how much of an increase there will be in the Von-Mises stress, to find the stress in the shear keys of FER, and in the case of NET, to see if they exceed the capacity of friction between adjacent coils. They are also compared to a cyclic stress allowable.

In this report nomemclature used by the FER team is adopted. The term "outer ring" means the part of the coil case on the side of the winding pack farthest from the plasma. The term "inner ring" means the part of the coil case on the side of the winding pack closest to the plasma. The side plates are the case parts next to the remaining sides of the winding pack. The "inner leg" of the coil is the straight part closest to the machine centerline.

2. Stresses from In-plane Loads

The first step is to estimate the stresses resulting from in-plane loads for both machines. The NET double null machine and the 1986 Advanced Option C FER are the selected options. Some parameters are shown in Table 1, and Figs. 1 & 2 show each machines' TF coil configurations. A sectional view of the inner legs at mid-plane can be seen in Fig. 3. NET has a significant advantage in radial thickness and in overall current density by not having a bucking cylinder.

Constant tension behavior for both machines is assumed. In both cases the coil shapes deviate from true constant tension shape, but their designs are intended to produce constant tension behavior by appropriately adjusting the stiffness of the structure around the coil perimeter. The achievement of this for both is considered apriori for this study.

The well known equations for the centering force F_x <N/m> and vertical separating force F_z <N> on the inner leg of a constant tension coil are:

$$F_x = 2\pi R_i \frac{B_{t_{max}}^2}{2\mu_0 N} \qquad F_z = \frac{1}{2}\frac{\mu_0 N I^2}{4\pi}\ln(R_2/R_1) \qquad (1,2)$$

These are both used for the FER device, but the centering force for NET had been calculated by the NET team using a magnetics program, and the value for F_x given in ref. 1 is used. It differs only slightly from the constant tension value. The values used for both machines are also shown in Table 1.

A key difference between the two machines, related to the bucked vs. wedged difference, is the design and use of the winding pack to sustain loads on the coil. The conductor cross sections can be seen in Fig. 4. The type of conductor used in FER has somewhat loosely twisted conductor strands inside the steel conduit, so only the conduit is capable of sustaining loads any direction, axial or transverse. It has a high conductor current density compared to the NET conductor, 33.0 A/mm^2 versus 21.6 A/mm^2. The NET conductor examined in this analysis is the SIN design, but it is noted that other designs are being considered for NET. The conductor strands are wound into a Rutherford cable, and on either side of the cable are solid pieces of stabilizing material, with helium cooling channels in the corners. Solder fills the voids around cable and between the stabilizers. This approach to the conductor design, though relatively low in conductor current density, provides greater load capacity in the axial and the Y (or toroidal) directions. This goes well with the wedging concept, since the winding pack will be compressed in the toroidal direction. Estimating the effectiveness of the winding pack in reacting coil loads is a required step for both machines. Equivalent Young's moduli of the winding pack are needed, as well as some appropriate assumptions about the manner in which the winding pack and coil case strain together.

In the vertical direction, it was first assumed that the coil case and the winding pack strained equally, but there was some concern over considerations that the conductor would not strain uniformly. One reason this would occur is because as the winding pack dilates from the in-plane loads, the inner conductors (those closest to the plasma)

would tend to strain more than the outer ones, especially if the insulation between turns is soft. Another reason is that the toroidal field across the winding pack is not uniform, and so the force across it would also not be uniform. Several schemes were tried to model this effect, which indicated small changes, but confidence was low in them. Still another concern was that the winding pack as a whole would strain more than the coil case because of gaps between the winding pack and case, or because of the soft insulation and epoxy between them. The Euratom LCT coil reportedly (ref. 2) had good success in filling such gaps with epoxy filled bladders since there was good force transmission between the winding pack and case. NET magnet team members have confidence in avoiding such gaps, but the FER team does not. In any case, by assuming (pessemistically) that such a gap existed between the winding pack and outer case ring, the effect still was small. Since it is primarily desired to estimate the coil case stresses, and since the effects of both of these concerns only decrease the case stress (at the expense of winding pack stress) a uniform strain assumption is adopted across the winding pack and case.

It should be stated that the stresses obtained in the winding pack are considered to have a larger error than those in the coil case. These effects, and others, probably will occur to some degree. Treatment of the winding pack as a homogenous continuum with equivalent Young's moduli is most useful in determining case stresses, but it is not believed to faithfully model the deformation in the winding pack itself. This would apply to finite element analysis also that use equivalent Young's moduli and treat the winding pack as a continuum.

2.1 Wedge TF coil Design of NET

Area mixture rules were used to determine the equivalent Young's moduli in the axial (Z) and toroidal (Y) directions.

The rectangular winding pack area shown in Fig. 5 has the two inboard corners cut for the three less turns there, and its area is 0.4017 m^2. There are 24 pancakes of twenty turns each, except for the two end pancakes which have 17, making a total of 474 turns. The total area of stainless steel conduit is 0.1288 m^2, and the stabilizer plus Rutherford cable is 0.1433 m^2. The assumed value for the modulus of stainless steel is 200. GPa, and that of stabilizer and Rutherford

cable 100. GPa. The contribution to the axial or Z stiffness is considered negligible for solder, insulation and epoxy filler. The resulting equivalent modulus for the winding pack area (which includes the ground insulation) was 100 GPa.

The coil case area is 0.1996 m^2. Using the vertical separating force on the inner leg of F_z = 74.8 MN, and using the respective areas and moduli, the total vertical strain was 0.0935 %. This corresponds to 187 MPa in the case and steel conduit, and 93.5 MPa in the superconductor and stabilizer. It works out that the winding pack reacts 50 % of the total vertical separating force. To repeat, the key assumptions used are the constant tension and uniform strain ones.

The Y direction modulus is estimated in steps. Again referring to Fig. 4, only the conduit wall and the marked area of the stabilizer shown is considered to bear load in this direction. The Rutherford cable and solder have a gap between them and the conduit, and solder is quite soft. The conduit wall and marked stabilizer area are assumed to strain uniformly in the Y direction along the length of the stabilizer (20.1 mm) and they react the load in parallel with each other. The stiffness contribution from insulation and epoxy along this length is neglected. The X dimension of the winding pack is 0.5648 m, so for 20 turns of 3.0 mm thick conduit and 3.1 mm stabilizer, we have for this first step:

$$20 \times 2 \times (0.003\times200 + 0.0031\times100)/0.5648 = 64.4 \text{ GPa}. \quad (3)$$

In constrast to this parallel model, the second step is a series model, since this 64.4 GPa modulus acts in series with the opposite conduit wall (those in the X-Z plane) plus the insulation and epoxy, over the Y dimension of the winding pack, 0.7152 m. The assumed modulus of insulation and epoxy is 20 GPa. Thus we have:

$$\frac{24\times2\times0.003}{200} + \frac{24\times0.0201}{64.4} + \frac{.7152-24\times(2\times.003+.0201)}{20} = \frac{0.7152}{E_{wpy}} \quad (4)$$

which results in E_{wpy} = 56.5 GPa.

Fig. 6 shows a static force diagram of the NET inner leg. The centering force is reacted by the X component of the force normal to the wedge surface, making the normal force easily determined at 116.1 MN/m. A Y component is also found: F_h = 113.9 MN/m. The model shown

in Fig. 6 is used to evaluate the toroidal compression. Some error is introduced by using a linear model as opposed to a curved one, but it should be small. In Fig. 6 the S_1 thickness is taken as an average of the case outer ring's thickness at the coil center and at the wedge surface, 0.154 m. S_2 is the winding pack X dimension: 0.5648 m. Again using a series model:

$$\frac{.7152/2}{56.5} + \frac{.4371 - .7152/2}{200} = \frac{.4371}{E_2} \tag{5}$$

giving E_2 = 65.0 GPa.

The boundary condition between adjacent coils is that the toroidal strain is a constant along the wedge surface. Applying this to the linear model of two columns under loads P_1 and P_2, where $P_1+P_2 = F_h$,

$$P_1 = \frac{F_h}{1+(S_2 \cdot E_2)/(S_1 \cdot E_1)} = 0.46\ F_h = 52.0\ \text{MN/m}, \tag{6}$$

and

$$P_2 = 0.54\ F_h = 61.9\ \text{MN/m}. \tag{7}$$

The linear strain is then $\varepsilon = (P_1/S_1)/(200\ \text{GPa}) = 0.169\ \%$. Using this as a toroidal strain, the inward radial displacement of the wedged coil is:

$$u_r = \varepsilon\ (1.78+(.154/2)) = 3.14\ \text{mm}. \tag{8}$$

This is in good agreement with the results of the two dimensional FEA obtained in reference 1 which gave 3.2 mm.

Looking at the outer ring, the compressive stress at the minimum thickness is 385 MPa, while at the coil edge it is 301 MPa. The average compressive stress of the winding-pack / side-plate region is 110 MPa. The discontinuity of stress where the case side plate meets the outer ring is a limitation of this model.

Friction between the winding pack and side plate plays an important role in the stresses of NET's case, but it is better to first consider the case of no friction. With no friction, the entire centering force is transferred to the case outer ring directly, and the side plates try to pull outwardly (in a relative sense) from the outer

ring as they become toroidally compressed. A tension is created between each side plate and outer ring, which has the effect of bending the outer ring. (Note that if the side plates had constant thickness and were not tapered, this tension force would not be created.)

To estimate this bending stress, the set of outer rings is modelled as a cylinder under the action of discrete loads, as in Fig. 7. Solutions for such problems are available (for example, ref.3). For this problem, two sets of loads are applied to the "cylinder", offset from each other by about 2 degrees, since the loads are assumed to act along a radial line through the middle of each side plate, and the two solutions superimposed. The magnitude of these loads is determined by considering that the other "cylinder", formed by the set of winding packs and side plates, developes its toroidal compression by being pulled inward by these side plate - outer ring forces, F_s. With this concept we get:

$$F_s = \pi P_2/16 = 12.15 \text{ MN/m} , \tag{9}$$

where 16 is the number of TF coils in NET. Interesting points for bending stresses in the outer ring are in the middle and at the ends. For the middle the bending moment is:

$$M_m = F_s R_o \left(\frac{\cos(\alpha)}{\sin(\theta)} - \frac{1}{\theta} \right) , \tag{10}$$

where R_o is the mean radius to the outer rings (1.78 + .154/2),
α is the angle between the wedge surface and the middle of the side plate, 0.01747 rad, and θ is the coil half angle, $\pi/16$.

Similarly, the bending moment at the end of the outer ring is:

$$M_e = F_s R_o \left(\frac{\cos(\theta-\alpha)}{\sin(\theta)} - \frac{1}{\theta} \right) . \tag{11}$$

The bending stresses are found by simply using:

$$\sigma = \frac{6M}{(1-\nu^2)\ t^2} \tag{12}$$

using the moment and thickness at the respective locations. The Poisson ratio (ν) used here is 0.29. The use of this model is valid provided the toroidal stress along the wedge surface remains in compression when

the bending stress is combined with the compressive stress -301 MPa found earlier.

Friction between the winding pack and side plates has the effect of directly transferring centering load from the winding pack to the side plates, and reducing the amount that is passed directly to the outer ring. Estimating the magnitude of the friction force transferred to the side plates is a difficult problem, because the mechanics of the friction phenomena under the actual conditions is not known, and because the deformation of the winding pack and its interaction with the coil case is not easily understood. The simplest of frictiom models is used here:

$$F_f = k_f \cdot P_2 \tag{13}$$

where k_f is a coefficient of friction。 Values of 0.0, 0.1, and 0.2 were tried. The side plate force F_s is reduced by the amount $F_f \cdot \cos(\theta-\alpha)$, and consequently so is the bending moment. Interestingly, at $k_f = 0.2$ (more precisely, $\theta/\cos(\theta-\alpha)$) the bending stress becomes zero, and hence it represents an optimum value of friction. Greater coefficients would cause an increase in bending moment, but in the opposite direction. The accuracy of the friction model is still questionable; consider also that if the coefficient was raised to 0.368 ($(F_x/2)/P_2$), it would imply that all of the centering force would pass through the side plates, and none would go directly to the outer ring. This seems quite unlikely. The bending model is reasonable though, and the strong sensitivity of bending moment to assumed friction coefficient is a cause for concern.

Bending and Von-Mises stresses at the middle and end of the outer ring are presented in Table 2 as a function of assummed friction coefficient. Points A and B can be seen in Fig. 5. At point A next to the winding pack, the X direction compressive stress is estimated by:

$$\sigma_x = (F_x - 2\, k_f\, P_2)/.7152 \quad . \tag{14}$$

The friction coefficient will also influence another potentially critical case stress. The force F_s between the side plate and outer ring passes through a minimum thickness near the side plate - outer ring junction (point C in Fig. 5). The thickness is approximately

0.041 m, so for k_f = 0.0, the tensile stress there is $F_s/0.041$ = 296 MPa. For k_f = 0.1, it is of course 148 MPa, and at k_f = 0.0 it is zero. This location is near the discontinuity in the toroidal compressive stress, and selecting the appropriate toroidal stress value for this location has uncertainty if we want to make a Von Mises estimate. If we use P_2/S_2 = -110 MPa, for k_f = 0.0, 0.1, and 0.2, we get Von Mises stresses of 364, 278, and 260 MPa, respectively. On the other hand, if we pessemistically use $P_1/S_{1_{end}}$ = -301 MPa, we would respecitvely get 551, 470, and 426 MPa. Local effects will be very important here.

NET conductor stresses:

An estimation can be made of the maximum stresses in the conductor conduit and stabilizer, but as mentioned earlier there is some greater uncertainty than with the case stresses. The strain and stresses in the Z direction have been solved already using the uniform strain assumption. In the X direction, it is assumed for both NET and FER that the centering force accumulates in the conduit walls (X-Z plane) only. This is most plausible for the FER conductor, but less so for NET's. It was adopted under the premise that the Rutherford cable and solder are ineffective in transfering load in the X direction. The maximum X stress in the conduit is in the row of turns closest to the outer ring, and is proportional to the value σ_x calculated above:

$$\sigma_{xc} = \sigma_x \ (.7152/(24\times.006))\times 19/20 \quad . \tag{15}$$

The first factor simply scales up the stress in proportion winding pack to conduit load bearing area ratio, and the second, nineteen out of twenty turns, is a reduction for last the row of conductors adjacent to the outer ring (possibly too strong considering the gradient of toroidal field across the winding pack).

In that last row the Y stress can be estimated by evaluating the strain in conduit/stabilizer section of the conductor shown in Fig. 4 which had the equivalent Y modulus of 64.4 GPa. That strain is:

$$\varepsilon_y = (P_2/.5648)/64.4 \text{ GPa} = 0.170 \ \% \tag{16}$$

which would mean for the conduit lying in the Y-Z plane, the Y compressive stress would be 340 MPa. At the corner of the conduit the X and Y stresses coexist (point D in Fig. 4), and here the maximum conduit Von Mises stress is found. These are presented in Table 3, again as a function of k_f:

Since the X stress in stabilizer is small under the assumptions used, the stabilizer's maximum Von Mises stress is independent of k_f. With σ_{ys} = 0.170 % × 100 GPa = 170 MPa, and σ_{zs} = 0.0935 % × 100 GPa = 93.5 MPa, the estimated maximum Von Mises stress is 231 MPa.

2.2 Bucked TF coil design of FER

The FER conductor design will support load only in the steel conduit. Using the assumption of uniform strain across the winding pack and coil case, the Z direction stress for the FER coil is a simple matter to estimate. The area of the coil case is 0.346 m^2, and the area of all the conduit from 286 conductor turns is 0.094 m^2, for a total of 0.440 m^2. The vertical separating force on the inner leg of FER is 68.3 MN, giving a Z stress of 155 MPa and a strain of 0.0776 %.

The load path of the centering load F_x is direct to the outer ring and bucking cylinder, and it is much simpler to estimate the stress from it than it is for NET. The Y width of the winding pack (subtracting out the ground insulation) is 0.660 m, so the X stress in outer ring is:

$$\sigma_x = 42.41/0.660 = 64.3 \text{ MPa} \quad . \tag{17}$$

In the conduit, this X stress is scaled up by the reduction in load bearing area, and then reduced for twelve out of thirteen turns:

$$\sigma_{xc} = \sigma_x \, (.66/(2\times22\times.035))\times12/13 = 254 \text{ MPa} \quad . \tag{18}$$

These are the stresses in the inner leg resulting from in-plane loads, ignoring any inhomogeneity of stress (to be discussed later). There are no Y direction stresses to consider. The maximum Von Mises stress in the outer ring case next to the winding pack is then 195 MPa, and in the conductor conduit in the row of conductors next to the outer ring it is 358 MPa.

3. Stresses from Out-of-plane Loads

3.1 NET

It is of particular interest for the NET machine to estimate the shear stress that develops between adjacent wedged coils, since this must be reacted by friction in the insulation layer between the coils. By doing this we will also estimate the shear stress in the coil itself. This problem was first approached by modelling the set of straight inner legs as two concentric cylinders with fixed ends, which twist from the distributed out of plane loading acting in them. They have equal rate of twist (and rotation angle) at any position along the length of the cylinders. The inside cylinder represents the set of outer rings, while the outside cylinder is for the set of winding packs with case side plates. The model has the limitation that there is a discontinuity of stress at the inside cylinder - outside cylinder interface, and that it is not able to indicate how the shear stress varies between the winding pack and side plate. It should give a reasonable estimate of the torsional deformation of the inner legs, and of the shear stresses.

The effect of the distributed out-of-plane load is approximated by dividing the composite cylinder length into equal segments, averaging the force per length at each end of each segment, and using that average as a constant value for the segment. NET's poloidal system is symmetric about the mid-plane of the device, so it is only needed to use half the straight inner leg length. Here we present the problem with the half length discretized into eight equal segments. The choice of eight is something of an arbitrary choice; more segments would improve the approximation, but it would also make for more calculation.

Fig. 8 shows the cylinder model. T_e is the reaction torque at the end, and T_m is the mid-plane reaction torque. The torque distribution created by the out-of-plane forces is redundantly reacted since only one of these end torques is needed for equilibrium. The theorum of least work (an energy method, see ref. 4, for example), is employed to solve for these reaction torques at each end of the cylinder. Only torsional strain energy is considered here. In applying the theorum to this model, we can say that the redundant reaction (in this case we have chosen T_e) assumes a value such that the strain energy is minimized. This also means that the change in torsional strain energy

with respect to a change in the redundant reaction is zero. We write this relation in the following integral form:

$$\frac{dU_T}{dT_e} = \int_{z=0}^{\ell} \frac{T_k}{GJ} \cdot \frac{dT_k}{dT_e} dz = 0 \qquad (19)$$

The shear modulus G and polar moment J are constant over the length, so they can be multiplied out of the equation. The integral is divided into eight segments. In each segment the torque T_k is considered constant, and its value is the end torque T_e minus the torque accumulated from the end through that segment. This makes each dT_k/dT_e equal one, and the intergral reduces to a simple linear equation with one unknown: T_e.

The force distribution was taken from ref. 5, Fig. 64, specifically at the time of the end of burn. From this distribution the average force per unit length is tabulated for each segment. Multiplying by the segment length, the number of coils, and the radius to the winding pack center gives the torque about the cylinder's axis created in each segment. The sum of torques accumulated from the cylinder end through each segment are then tabulated, and these sums are used in the linear equation to solve for T_e. T_m can be obtained from the equilibrium equation, but it is not needed for the value of torque in a given segment. The tabulated values can be seen in Table A1 in the appendix A. The value of T_e obtained is 927 MN-m, and the resultant torque in each segment is obtained by subtracting the value in column 4 from T_e. T_e itself has greater magnitude than any of these torques, so it is selected as the worst case for shear stress.

In order to estimate the shear stresses it is necessary to determine the fraction of torque reacted by the inside and outside cylinders. We use the condition of equal rate of twist at any Z position between the inside and outside cylinders. Thus we can write:

$$\frac{T_i}{J_i G_i} = \frac{T_o}{J_o G_o}, \quad \text{and} \quad T_i + T_o = T \quad . \qquad (20,21)$$

These are combined to give:

$$\frac{T_i}{T} = \frac{1}{1+(J_o G_o)/(J_i G_i)}, \quad \text{and} \quad T_o/T = 1 - T_i/T \qquad (22,23)$$

The most troublesome point in this is finding an appropriate value for G_o, the equivalent shear modulus of the outside cylinder. An appropriate value for the winding pack's shear modulus, and how to combine it with the side plates, is not clearly available. Several paths were tried to narrow the range of values. First, in ref. 1 a transverse Young's modulus of 77 GPa and a Poission's ratio of 0.33 were determined for the winding pack based on the 2-D finite element analysis of a quarter section of the SIN conductor. Although it is admittedly not a truthful application of the relation, if we use $G = E/(2(1+\nu))$ with these values we get $G_{wp} = 29$ GPa. There is still additional ground insulation and epoxy to account for across the winding pack cavity, and the side plate thickness as well. Using composite mixture rules (also of questionable basis) in the same way as in determining the value E_2 in section 2.1, we can arrive at $G_o = 27$ GPa. The procedure is shown with more detail in appendix A. Other estimates were made using composite mixture rules and different assumptions about which components in the conductor would carry the shear load, which resulted in estimates for G_o of 24, 28, and 32 GPa. Table 4 shows results based on each of these assumptions; it can be seen that the variation with the value of G_o is small and is probably smaller than the error from other uncertainties.

The shear stresses shown are based on T_e and use the relation $\tau = Tr/J$. The maximum value τ_{max} shown is the value at the outer radius of each cylinder; the average value τ_{ave} is to the mean radius of each cylinder.

These values agree well with NET team's own FEA results at the top of the straight part of the inner leg. Fig. 21 of ref. 5 indicates the shear stress to be about 35 MPa. The plotted values in Fig. 21 are the maximums from the four elements of the winding pack, and though it is not completely obvious, these values are assumed to be taken from the centroid of the elements. If we extrapolate to the edge of the winding pack (plasma side) this would increase the FEA result to 37 MPa.

After this analysis was first performed, there was some concern about the validity of using the fixed end boundary conditions on the composite cylinder. In an effort to substantiate its use, a more extensive hand analysis was done modelling the entire TF coil. The theorum of least work was again used, and the coil discretized in a

crude way. This time the half cylinder length was divided into three segments, and the remaining part of the coil above the mid plane was also divided into three parts of equal curvature. This required some deviation from the true coil shape where it meets the inner leg. Bending moment and torsion equations for each segment were written in terms of the applied out-of-plane loads, the reaction loads and the position in the segment. The intercoil structure strain energy was also included.

It should be obvious that this was a very time consuming and difficult hand analysis, and there would be little value in presenting the details here, other than giving the result. The shear stress at the top of the cylinder was reestimated to be:

outer rings : τ_{max} = 79 MPa, τ_{ave} = 76 MPa

winding-packs and side-plates: τ_{max} = 36 MPa, τ_{ave} = 32 MPa

This might indicate the fixed end condition gives a slightly high result. However, upon considering the vague estimates for bending and torsional stiffnesses that had to be used, the many approximating assumptions needed, and the possibililties for calculation error, it is surprising that the new result was as close to the others as it was. This analysis would not easily lend itself to programming for a systems code subroutine, and the large effort needed for such a small difference of low confidence is simply not worth any further effort.

3.2 FER

The above estimation technique can also be applied to the FER coil to estimate the stress in the shear keys. Unlike NET, FER is a single null divertor machine and its poloidal field coil system is not symmetric about the midplane, so the full length of the straight inner leg must be modelled. Otherwise, the technique for finding the maximum torque in the inner legs is the same.

A question about estimating the shear stresses for FER is the influence the bucking cylinder has in reacting some of the torsional load. The bucking cylinder is split along an axial line (to reduce eddy current lossess), so its torsional stiffness is not nearly as great as if it were continuous. Nevertheless it may give some

assistance to the coil in reacting the torsion.

Until that is understood better, we will assume that all of the shear must be reacted by the shear keys. The shear key configuration for FER-ACS has not been clearly defined, but by making some assumptions for the X depth of the keys, and the Z height and spacing, an estimate can be made. The X depth of the keys is assumed at 2.5 times the thickness of the case inner ring (case wall closest to the plasma), which comes to be 32.5 cm. The Z height and spacing assumed is a best case condition, which is the key height equals the space between the keys, so the shear stress in the keys is the same as the shear stress in the case between the keys (implying that the shear key stress is twice the value obtained if the full inner leg Z height were available to react the shear stress). It is also assumed that the keys have sufficient Z depth so that shear and not bending is the dominant mode in the keys. With these assumptions, the maximum shear stress in the keys is 66 MPa at the end of burn, and it occurs at the bottom of the inner leg where the torque was found to be 184.5 MN-m (at the end nearest to the divertor).

The shear stress in the keys is not likely to be a critcial issue for the bucked/keyed design, although local stresses in the case or keys, and/or the compressive bearing stress on the insulation (between the keys and coil case) will require examination in future detailed stress analyses.

4. Discussion of Results

Maximum stress intensity levels in FER and NET are strikingly different from the results obtained.

The relatively high overall current density and low radial thickness of the inner leg of NET are attractive features, however, the Von Mises stresses from the in-plane loads are quite high. Depending on the friction value used, they can exceed the allowable Von Mises set by the NET team of 600 MPa (ref. 6). The results obtained here are in good agreement with the two dimesional FEA performed in ref. 1; for example, the Von Mises stress at point B in the outer ring (also point B in Fig. 2 of ref. 1) was found to be 540 MPa here, versus 566 MPa in ref. 1, for $k_f = 0.1$. The conductor conduit maximum Von Mises stresses agree well also, but the stabilizer estimate was about 20 %

assistance to the coil in reacting the torsion.

Until that is understood better, we will assume that all of the shear must be reacted by the shear keys. The shear key configuration for FER-ACS has not been clearly defined, but by making some assumptions for the X depth of the keys, and the Z height and spacing, an estimate can be made. The X depth of the keys is assumed at 2.5 times the thickness of the case inner ring (case wall closest to the plasma), which comes to be 32.5 cm. The Z height and spacing assumed is a best case condition, which is the key height equals the space between the keys, so the shear stress in the keys is the same as the shear stress in the case between the keys (implying that the shear key stress is twice the value obtained if the full inner leg Z height were available to react the shear stress). It is also assumed that the keys have sufficient Z depth so that shear and not bending is the dominant mode in the keys. With these assumptions, the maximum shear stress in the keys is 66 MPa at the end of burn, and it occurs at the bottom of the inner leg where the torque was found to be 184.5 MN-m (at the end nearest to the divertor).

The shear stress in the keys is not likely to be a critcial issue for the bucked/keyed design, although local stresses in the case or keys, and/or the compressive bearing stress on the insulation (between the keys and coil case) will require examination in future detailed stress analyses.

4. Discussion of Results

Maximum stress intensity levels in FER and NET are strikingly different from the results obtained.

The relatively high overall current density and low radial thickness of the inner leg of NET are attractive features, however, the Von Mises stresses from the in-plane loads are quite high. Depending on the friction value used, they can exceed the allowable Von Mises set by the NET team of 600 MPa (ref. 6). The results obtained here are in good agreement with the two dimesional FEA performed in ref. 1; for example, the Von Mises stress at point B in the outer ring (also point B in Fig. 2 of ref. 1) was found to be 540 MPa here, versus 566 MPa in ref. 1, for $k_f = 0.1$. The conductor conduit maximum Von Mises stresses agree well also, but the stabilizer estimate was about 20 %

low. For the conduit, here we have estimated 507 MPa, versus 500 MPa in ref. 1, and for the stabilizer, we have 231 versus 295 MPa (for k_f = 0.0. Results for the coil conductor components were not presented in ref. 1 for k_f = 0.0; the conductor component stresses presented appear to be independent of k_f.) The two dimension FEA also recommended that the outer ring (or inner vault in their nomemclature) would benefit from increased thickness. Three dimensional FEA results (ref. 6) of the entire NET coil found a maximum Von Mises in the case outer ring of 525 MPa, but this result is obtained with a no-slip condition between the winding pack and coil case. It is also mentioned in that report that the course mesh may be underestimating the maximum stress, and that the outer ring thickness possibly should be changed beacause of a mismatch of stiffnesses between the winding pack and case. The question of friction between the winding pack and coil case is discussed in ref. 6 only in how it effects the winding pack, but we believed that this friction question must also be investigated in that it can strongly effect the bending stress in the outer ring, and the tensile stress at the outer ring - side plate junction.

As mentioned in section 2.1, a coefficient of 0.2 represents an optimum value where bending in the outer ring becomes neglible. For different reasons, k_f = 0.2 is also considered optimum in the report by Marinucci and Wassermann (ref. 1), where it is presented as giving an ideal bond or no-slip condition between the winding pack and side plate. Using optimum assumptions about this friction phenomena may be indicating acceptable stress levels when they are excessive. Simple models cannot, and finite element codes may not be able to accurately model the true friction behavior and winding pack - coil case interaction under operating conditions. It would be prudent to design to more conservative friction assumtions until this can be done with confidence.

The estimated shear stress found in the winding pack - side plate region also agreed well with the NET teams own 3-D FEA (ref. 5) at the top of the inner leg. The maximum value of 37 MPa must be reacted by friction between adjacent coils, and this may be too high as indicated in refs. 5 and 6. 30 MPa is the chosen design limit, so there might be some slipping between coils or damage to insulation.

The FER coil is at the opposite extreme of stress intensity. Albeit with only in-plane being considered, a maximum Von Mises stress

in FER's coil case of 195 MPa is an inefficient use of structural material. The radial thickness of the inner leg plus bucking cylinder, and the overall current density are relatively poor because of this. The structural reliability of the coil is of the utmost importance, but a minimum thickness TF inner leg will help keep the overall radial build of the machine as small as possible. Further optimization is needed. (It has in fact begun with FER-ACS-M, or modified ACS).

To be fair, local stresses from out-of-plane forces have played a driving role in sizing the case thicknesses of FER. Algorithms for these stresses that the FER team have used (ref. 7) are being reviewed and updated for appropriateness and accuracy. These have been incorporated in the program subroutine for the bucked type magnet option.

The bucking cylinder hoop stress is -352 MPa, based on a thin wall cylinder model. The critical buckling stress is -552 MPa based on elastic stability limits for a cylinder under pressure, with a saftey factor of three, so there appears to be room for reducing the bucking cylinder thickness as well. In reviewing this critical stress some questions have been raised which concern both FER and NET. The use of a cylinder model under pressure is questionable for three reasons: The loading of the coils is more like centering force than pressure. A critical stress solution is available for cylinders under centering force, which is higher than the critical stress for pressure by a factor of 4/3 (force always acts to the center of the cylinder, even after buckling begins, versus pressure which acts always normal to the surface). Even then the centering force is not uniformly distributed over the surface of the cylinder; The bucking cylinder has non-uniform thickness; Most importantly, the bucking cylinder is split axially with an insulation break inserted to reduce eddy current losses.

The question was then asked as to what stability limit should be considered for the NET coil. If the inner legs are considered as a cylinder, then it has 16 axial splits versus only one. The cylinder model for buckling is not likely to be even remotely applicable. The issue of elastic stability limits for both FER and NET should be studied further, both for normal operating conditions and for some fault conditions, such as one coil dumping.

If the FER coil is further optimized to make better use of the structural material, and the NET coil's stresses reduced to a safer

value, the radial thickness and overall current density of the two machines might become comparable. The buckling stability criteria may become an important factor in choosing a bucked or wedged configuration.

II. TF Stress Subroutine for Use in System Codes Modelling

1. Goals of the Subroutine

It was desired to provide new capabilities to the original TF stress subroutine in TRESCODE and to review and improve it where possible. The original subroutine did not have capability for estimating stresses in a wedged type coil such as NET. For bucked type coils, the conduit in the winding pack was not included for reacting some of the vertical separating force. Also, one of the algorithms for local bending stress in the outer ring was judged inappropriate for the inner leg, since it applied to a region of the coil away from the straight inner leg, and it was decided to omit it.

The local stresses due to out-of-plane force were based on a maximum poloidal field in the TF coil. The original TRESCODE subroutine was executed before the poloidal coil scenario is determined, so an initial guess for the value of Bp_{max} (poloidal field in TF winding pack) was needed as an input to get a maximum out of plane force. There were two problems with this. One is that if the code is not operated in an iterative mode, the initial guess is not checked and modified. The second is that the value of Bp_{max} used (initial guess or code calculated) is the maximum found on the whole coil, and not necessarily on the inner leg. Typically the maximum occurs in the curved part of the coil just above or below the straight inner leg. Using that maximum force to size the inner leg case is not appropriate; the case can be thicker near those maximum force regions without penalizing the radial build.

Since it is preferable to use calculated out-of-plane forces, any stresses from those forces will need to be estimated after the poloidal field scenario is determined (i.e., the MHD calculations are finished). Further, since it is not known apriori at which stage of the operation cycle the highest stresses will occur, the worst case

value, the radial thickness and overall current density of the two machines might become comparable. The buckling stability criteria may become an important factor in choosing a bucked or wedged configuration.

II. TF Stress Subroutine for Use in System Codes Modelling

1. Goals of the Subroutine

It was desired to provide new capabilities to the original TF stress subroutine in TRESCODE and to review and improve it where possible. The original subroutine did not have capability for estimating stresses in a wedged type coil such as NET. For bucked type coils, the conduit in the winding pack was not included for reacting some of the vertical separating force. Also, one of the algorithms for local bending stress in the outer ring was judged inappropriate for the inner leg, since it applied to a region of the coil away from the straight inner leg, and it was decided to omit it.

The local stresses due to out-of-plane force were based on a maximum poloidal field in the TF coil. The original TRESCODE subroutine was executed before the poloidal coil scenario is determined, so an initial guess for the value of Bp_{max} (poloidal field in TF winding pack) was needed as an input to get a maximum out of plane force. There were two problems with this. One is that if the code is not operated in an iterative mode, the initial guess is not checked and modified. The second is that the value of Bp_{max} used (initial guess or code calculated) is the maximum found on the whole coil, and not necessarily on the inner leg. Typically the maximum occurs in the curved part of the coil just above or below the straight inner leg. Using that maximum force to size the inner leg case is not appropriate; the case can be thicker near those maximum force regions without penalizing the radial build.

Since it is preferable to use calculated out-of-plane forces, any stresses from those forces will need to be estimated after the poloidal field scenario is determined (i.e., the MHD calculations are finished). Further, since it is not known apriori at which stage of the operation cycle the highest stresses will occur, the worst case

must be found among each stage: ignition approach, beginning of burn, and end of burn (the plasma breakdown stage always has much lower poloidal currents).

For this reason, the new subroutine is divided into two stages; the inplane stresses are estimated before the poloidal scenario is determined, and the out-of-plane stresses are done after. Combined results (maximum Von Mises stresses) are also done later.

As implied, maximum Von Mises stress will used as a stress intensity criteria. Cyclic stresses from out-of-plane forces will also be checked against an allowable value in the new subroutine. These include the local stresses in the coil case (for bucked type) and shear stresses from torsion of the inner leg (bucked and wedged types). Where appropriate, these are combined to obtain a principal stress which is compared to the cyclic allowable.

It was considered to provide some methodology for optimizing the coil case thicknesses. Such a scheme should be able to identify excessive stresses and make an adjustment in case thickness in response to the level of excess and its location. It could also optimize on the basis of too low levels of stress, such as the working stress being less than 50 % of the allowable. Some iteration would be involved, before and/or after the PF scenario is determined in the code. Developing such a methodolgy will not be an easy task, and there was not sufficient time for this work to give it a serious effort. Some features of the subroutines were put in with this optimization task in mind, so future programers would have them available when the work can be pursued.

2. Coding of Analysis Methods

2.1 In-plane stresses

The coding for in-plane stresses follows the logic outlined in Part I exactly. The value of maximum field as it enters the module is determined by Ampere's Law and has been multiplied by a correction factor which accounts for the effect of field ripple on the TF winding pack. This is used in another subroutine for superconductor analysis, but it needs to be divided out for dertermining the centering force, F_x.

The beginning of the first subroutine module evaluates the allowable Von Mises stress. It chooses the minimum of two-thirds of the yield strength or one-half the ultimate strength of the coil case material. A safety factor is applied by user input.

The module's logic then branches into either a bucked type magnet or wedged type. For the bucked type, the bucking cylinder allowable stress is set as the minimum of 2/3 yield strength, 1/2 ultimate, or the critical stress based on the elastic stability of a thin wall cylinder under centering force (with a safety factor of 4).

Wedged type coils required an input value for E_{wpy} (eqn. 4) from the user. It will depend on the conductor design and winding pack layout being used, so an estimate of it should be made by hand for different types of conductor. It is not used for bucked type coils. The code will evaluate the value of E_2 (eqn. 5) for the combined winding pack - side plate region.

Stresses are evaluated as described in Part I, and are written to output. Case stresses (and the bucking cylinder stress) are checked against the allowable, and if they exceed it, a flag is set. There is a separate flag for each location, so if optimization is to be done later, the specific location can be identified. Examples of output from the in-plane subroutine module as executed in TRESCODE can be seen in appendix B for both a bucked machine and a wedged machine. The machine for the bucked case is FER ACS-M (Advanced Option C - Modified); the wedged example is the double null NET machine. The results do not exactly match those as presented in part I because the ACS-M machine is slightly different than the ACS one, and simulation of NET by TRESCODE does not give exactly the same configuration as analyzed in Part I. Before merging the subroutines into TRESCODE, they were verified in a stand alone mode with the same input values used in the hand analyses.

The allowable Von Mises stress is lower than what is now being used by the design teams. The in-plane results for NET violated that allowable at two locations checked in the case. The example shown used a winding pack - side plate friction coefficient of 0.00, so the result is the most conservative. FER stresses are significantly lower than the allowable.

The end of the in-plane module might be a good location for a first pass at optimizing the case thickness. If stresses are too high

(or too low), an adjustment and iteration could be made before the PF scenario is determined (with CPU time consuming MHD calculations). However, it may be that the out-of-plane stresses will be more limiting than the in-plane, so it not obvious what the best strategy for optimization is.

2.2 Out-of-plane stresses

The out-of-plane module estimates shear stresses from torsion of the inner legs, and local bending stresses in the case of a bucked type coil. The worst condition of torsional shear stress needs to be found by checking the torque at different Z positions along the length of the strainght inner leg, and checking them at the ignition approach, beginning of burn, and the end of burn times of the operation scenario. There is a loop over each of the times. Then for each time, the equations derived from applying the theorum of least work are used to determine the reaction torque at the top of the cylinder (it uses the fixed end condition assumption). The out-of-plane forces (per unit length) are determined in the PFONTF subroutine, which gives the running load values at the ends of ten equal segments of the straight inner leg. They are stored for each time in the operation cycle. The logic for determining the torque at the top is the same as was described in Part I except the discretization of the inner leg is ten instead of eight. The running loads at each segment end are averaged and multiplied by the segment length to get a force for that segment. (These could be multiplied by the radius to the middle of the winding pack and the number of TF coils at this time to get torque values, but this is postponed until later since it is not needed to solve the energy equation.) At each segment, the sum of the accumulated force in that segment is subtracted from the top reaction to get the resultant for that segment. The magnitude of these are successively compared to find the maximum; the approximate Z position of the maximum and the time when it occurs is saved in addition to the value itself. By multiplying by the winding pack radius and number of coils we get the torque. For each operation time, the torques at the top, bottom and mid-plane of the inner leg are used; the maximum value is used after all times have been checked.

Depending on the type of coil being analyzed, the use of the torques is different. For FER type coils, all of the torque at a given Z position is assumed to be carried by the inner ring of the case. The polar moment of inertia for the inner ring radius and thickness is calculated at beginning of the module, and it is used with the torque and mean radius of the inner ring to estimate the shear stress in it. Stress values at the top, bottom and mid-plane are output for each operation time. The maximum inner ring shear stress with its position and time are listed afterwards. Shear key maximum stress is estimated by assuming a radial thickness of the key 2.5 times the inner ring thickness (which could easily be adjusted). A polar moment of inertia using that thickness and radius to the keys is calculated, and a shear stress from that. This value is finally multiplied by two, to account for the reduced shear load bearing area in the Z direction. Two corresponds to equal key height and spacing between keys, as mentioned in section 3.2.

The torque in the NET coil is shared between the outer ring and winding pack - side plate (corresponding to the inside and outside parts of the composite cylinder model). The shear modulus for the outer rings is taken from steel's Young's modulus and Poission's ratio, but there is no good algorithm for the shear modulus of the winding pack - side plate region. For lack of a better one, the value of E_2 which is calculated from the input value of E_{wpy} (see section 2.1) is used with a fictitious Poission's ratio to get an equivalent shear modulus. At this point the ratio is set at 0.15 to give a shear modulus of about 28 GPa for NET, but it should be adjusted depending on the conductor design and winding pack layout. The fraction of torque reacted is determined as in equations 23 and 24 (section 3.1). The stresses are estimated based on the polar moment of inertia of the inside or outside cylinders (outer rings or w/p - s/p), the amount of torque carried by the respective cylinder, and the mean radius of the cylinder. Stresses for each operation time are output at the top, bottom and mid-plane of the inner legs. The maximum shear stresses are printed last, with its position and time.

Shear stresses are compared to a cyclic allowable, which is a user input based on Mode I fatigue crack growth analysis. This is adopted under the premise that the principal stress from the shear will be limited by the allowable in the same way a tensile normal stress would be.

Local stresses from the out-of-plane forces are estimated for bucked type coils. All but one of the algorithms from the original TRESCODE TF stress subtoutine are used. These provide estimates of stresses for: bending plus tension of the outer ring, near the winding pack corner; bending plus tension of the inner ring, near the winding pack corner; bending at the middle of the side plate (see Fig. 5 for these positions). The maximum out-of-plane force from the PFONTF subroutine is found along with its position and time. After the operation time loop is completed, these stresses are listed. They are compared against the cyclic allowable stress. In addition, the maximum local stress in the inner ring is combined with the shear stress in the inner ring to get a principal stress, which is then compared to the cyclic allowable (using shear stress based on the torque at the position and time of maximum out-of-plane force, since the maximum out-of-plane force and maximum torque do not necessarily coincide in position or time). Finally, the maximum shear stress in the inner ring is combined with the local stress in the inner ring, based on the position and time of maximum torque, and that principal stress is compared against the allowable cyclic stress.

There is no estimation of local stress from out-of-plane forces for wedged type coils.

Von Mises stresses from the in-plane force will be increased by the shear stresses in both type of coils, and bucked types will additionally be effected by the local stresses. The out-of-plane module reestimates the Von Mises stresses at the same location of the inner leg cross section as in the in-plane module. For wedged type coils this means the outer ring Von Mises stresses (points A and B in Fig. 5) are checked by combining the in-plane results with the maximum shear stress found in the outer ring. . The Von Mises stress at the side plate location has the maximum shear stress in the winding pack - side plate combined with the in-plane stresses.

Bucked coils do not have the outer ring Von Mises stress rechecked, since under the assumptions used the shear stress is zero. New Von Mises stresses are checked though. The stress from the maximum out-of-plane force is used at four points. At each of these points the vertical stress is combined with the other stresses there. These points and stresses are (see Fig. 5):

(1) in the outer ring near the winding pack corner,
with the bending plus tension stress there,
plus the centering pressure from the winding pack;
(2) in the side plate next to the winding pack,
the bending stress, plus the out-of-plane pressure;
(3) in the side plate at the case edge away from the winding pack,
the bending stress;
(4) in the inner ring near the winding pack corner,
the bending plus tension stress, plus the shear stress.

The inner ring position (4) is also checked by combining the vertical stress, the maximum shear stress, and the out-of-plane bending plus tension stress (out-of-plane force from position and time of max. shear). Each of these are compared to the allowable Von Mises stress.

If any of the estimated stresses exceed the allowable, Von Mises or cyclic, a flag is set for the specific condition, and a message is printed to output.

One final stress estimate is made for both types of coil. It is based on a worst assumption that the torsional restraint, either the shear keys for bucked type, or friction between adjacent coils for wedged type, fails completely, and the inner leg bends from the out-of-plane forces. A fixed end beam model is used, using ten loads applied at the middle of each of the discretized segments of the inner leg. This estimate is the least accurate of all performed, and it is presented for information only. No checks are made against any allowable. The highest bending moment on the inner leg is found by using an energy method, and checking each operation time and position along the length of the inner leg. Once that is found, the maximum bending stress in the coil case is estimated by using the fraction of bending moment reacted by the case. It is assumed that the case and winding pack strain equally at each Z position. The fraction is:

$$FSHRC = 1/(1 + E_{wpz} \cdot AMOD_{wp})/(E_{steel} \cdot AMOD_{cs})) \qquad (24)$$

where

E_{wpz} is the winding pack Z direction modulus,
$AMOD_{wp}$ is the X-X area moment of inertia of the winding pack,
E_{steel} is the Young's modulus of steel
$AMOD_{cs}$ is the area moment of inertia of the case.

Appendix B contains the stage two output from TRESCODE for the two trial cases. In addition to the out-of-plane stresses, the reevaluated Von Mises stresses are shown. In the NET output, a message is printed indicating the Von-Mises allowable has been exceeded at two locations.

3. Summary and Desired Subroutine Improvements

The two stage approach to estimating TF coil stresses for TRESCODE systems studies provides more accurate results for both bucked and wedged type magnets without requiring excessive computing time. The winding pack's contribution to reacting some of the loading is accounted for in the stress estimates. The actual out-of-plane force distribution over the inners legs is employed to estimate torsional shear stresses for both types of coils, and coil case bending stresses for bucked type coils. Shear stresses and bending stresses are checked against a cyclic allowable stress limit. Von-Mises stresses are determined at several critical locations in the coil case, combining the effects of both in-plane and out-of-plane loads. These are compared to an allowable Von-Mises stress limit.

To expand the usefulness of systems studies, additional types of coil configurations should be accomodated by the stress subroutines in addition to bucked and wedged, for example, the hybrid bucked-wedge configuration such as proposed for TIBER.

It is desired that an optimization capability be added to the stress subroutines to help produce a minimum radial thickness of the inner leg. To fulfill this task it be necessary to change the coil's dimensions in response to the most limiting stress condition, which must be found from all of the obtained results. Further, the optimization feature should change coil dimensions in response to both excessively high stresses, and excessively low stresses.

An improved buckling limit for the bucked option is desired, and one may be needed for the wedged option.

Appendix B contains the stage two output from TRESCODE for the two trial cases. In addition to the out-of-plane stresses, the reevaluated Von Mises stresses are shown. In the NET output, a message is printed indicating the Von-Mises allowable has been exceeded at two locations.

3. Summary and Desired Subroutine Improvements

The two stage approach to estimating TF coil stresses for TRESCODE systems studies provides more accurate results for both bucked and wedged type magnets without requiring excessive computing time. The winding pack's contribution to reacting some of the loading is accounted for in the stress estimates. The actual out-of-plane force distribution over the inners legs is employed to estimate torsional shear stresses for both types of coils, and coil case bending stresses for bucked type coils. Shear stresses and bending stresses are checked against a cyclic allowable stress limit. Von-Mises stresses are determined at several critical locations in the coil case, combining the effects of both in-plane and out-of-plane loads. These are compared to an allowable Von-Mises stress limit.

To expand the usefulness of systems studies, additional types of coil configurations should be accomodated by the stress subroutines in addition to bucked and wedged, for example, the hybrid bucked-wedge configuration such as proposed for TIBER.

It is desired that an optimization capability be added to the stress subroutines to help produce a minimum radial thickness of the inner leg. To fulfill this task it be necessary to change the coil's dimensions in response to the most limiting stress condition, which must be found from all of the obtained results. Further, the optimization feature should change coil dimensions in response to both excessively high stresses, and excessively low stresses.

An improved buckling limit for the bucked option is desired, and one may be needed for the wedged option.

Acknowledgements

The authors wish to extend their gratitude to H. Iida, T. Horie, F. Iida, K. Toyoda, Y. Wachi, M. Konno, and T. Mizoguchi, for giving valuable guidance and discussions in the course of this work. They also would like to acknowledge Drs. S. Tamura, M. Yoshikawa, and K. Tomabechi for providing support and encouragement.

References

1. C. Marinucci, C.U. Wassermann, "Stress Analysis of the SIN Conductor the NET TF-Coil", Proc. of the Thirteenth Topical Meeting on the Technology of Thermonuclear Fusion, 1819 (1986)
2. H. Tsuji, et al., "Experimental Results of Domestic Testing of the Pool-boiling Cooled Japanese and the Forced-flow Cooled EURATOM LCT Coils", Cryogenics, October 1985, Vol. 25, p539
3. R.J. Roark, W.C. Young, "Formulas for Stress and Strain", 5th ed., McGraw-Hill Book Co., 1982, Table 17, No. 7
4. J.T. Oden, "Mechanics of Elastic Structures", McGraw-Hill Book Company, 1967
5. R. Gori, N. Mitchell, H. Gorenflo, L. Ingala, "Structural Analysis of a NET Toroidal Field Coil Under Normal Operating Conditions, Part I", November 1987, NET/IN/87-07
6. N. Mitchell, et al., "Structural Assessment of the NET Toroidal Field Coils", March 1987, NET/IN/86-061 (k1), EUR-FU/XII-80/87/69
7. N. Miki, et al., "Conceptual Design Study of Fusion Experimental Reactor (FY86 FER) ---Magnet Design---", Sept. 1987, JAERI-M 87-153, sect. 2.6.2, in Japanese

Acknowledgements

The authors wish to extend their gratitude to H. Iida, T. Horie, F. Iida, K. Toyoda, Y. Wachi, M. Konno, and T. Mizoguchi, for giving valuable guidance and discussions in the course of this work. They also would like to acknowledge Drs. S. Tamura, M. Yoshikawa, and K. Tomabechi for providing support and encouragement.

References

1. C. Marinucci, C.U. Wassermann, "Stress Analysis of the SIN Conductor the NET TF-Coil", Proc. of the Thirteenth Topical Meeting on the Technology of Thermonuclear Fusion, 1819 (1986)
2. H. Tsuji, et al., "Experimental Results of Domestic Testing of the Pool-boiling Cooled Japanese and the Forced-flow Cooled EURATOM LCT Coils", Cryogenics, October 1985, Vol. 25, p539
3. R.J. Roark, W.C. Young, "Formulas for Stress and Strain", 5th ed., McGraw-Hill Book Co., 1982, Table 17, No. 7
4. J.T. Oden, "Mechanics of Elastic Structures", McGraw-Hill Book Company, 1967
5. R. Gori, N. Mitchell, H. Gorenflo, L. Ingala, "Structural Analysis of a NET Toroidal Field Coil Under Normal Operating Conditions, Part I", November 1987, NET/IN/87-07
6. N. Mitchell, et al., "Structural Assessment of the NET Toroidal Field Coils", March 1987, NET/IN/86-061 (kl), EUR-FU/XII-80/87/69
7. N. Miki, et al., "Conceptual Design Study of Fusion Experimental Reactor (FY86 FER) ---Magnet Design---", Sept. 1987, JAERI-M 87-153, sect. 2.6.2, in Japanese

Table 1 TF coil parameters for the NET and FER

	NET	FER
R_0 <m>	5.18	4.42
B_t <T>	5.00	4.61
I_p <MA>	10.8	8.74
R_1 <m>	2.198	1.845
R_2 <m>	8.833	8.950
R_i <m>	2.48	2.04
No. TF coils	16	12
Current/coil <MAT>	8.09	8.49
F_x <MN/m>	45.3	42.41
F_z <MN>	74.8	68.3
divertor	double null	single null

R_1 is radius to inner leg winding pack center;
R_2 is radius to outer leg winding pack center;
R_i is radius to inner leg winding pack position of maximum field

Table 2 NET bending and Von-Mises stresses from in-plane loads

k_f	Bend. at A	Bend. at B	V-M at A	V-M at B
0.0	-260 MPa	-242 MPa	739 MPa	657 MPa
0.1	-130 MPa	-121 MPa	619 MPa	540 MPa
0.2	0 MPa	0 MPa	500 MPa	426 MPa

Table 3 Maximum Von-Mises stress in NET conductor conduit

k_f	σ_{xc} at D	σ_{yc} at D	V-M at D
0.0	-298 MPa	-340 MPa	507 MPa
0.1	-217 MPa	-340 MPa	476 MPa
0.2	-136 MPa	-340 MPa	460 MPa

Table 4 Estimated shear stresses in NET inner legs

	G_o (GPa)	24	28	32
Outer rings (Inside cyl.)	T_i/T	.3078	.2759	.2501
	τ_{max} (MPa)	102	91	83
	τ_{ave} (MPa)	98	88	80
Winding-packs and side-plates (Outside cyl.)	T_o/T	.6922	.7241	.7499
	τ_{max} (MPa)	40	42	41
	τ_{ave} (MPa)	35	37	38

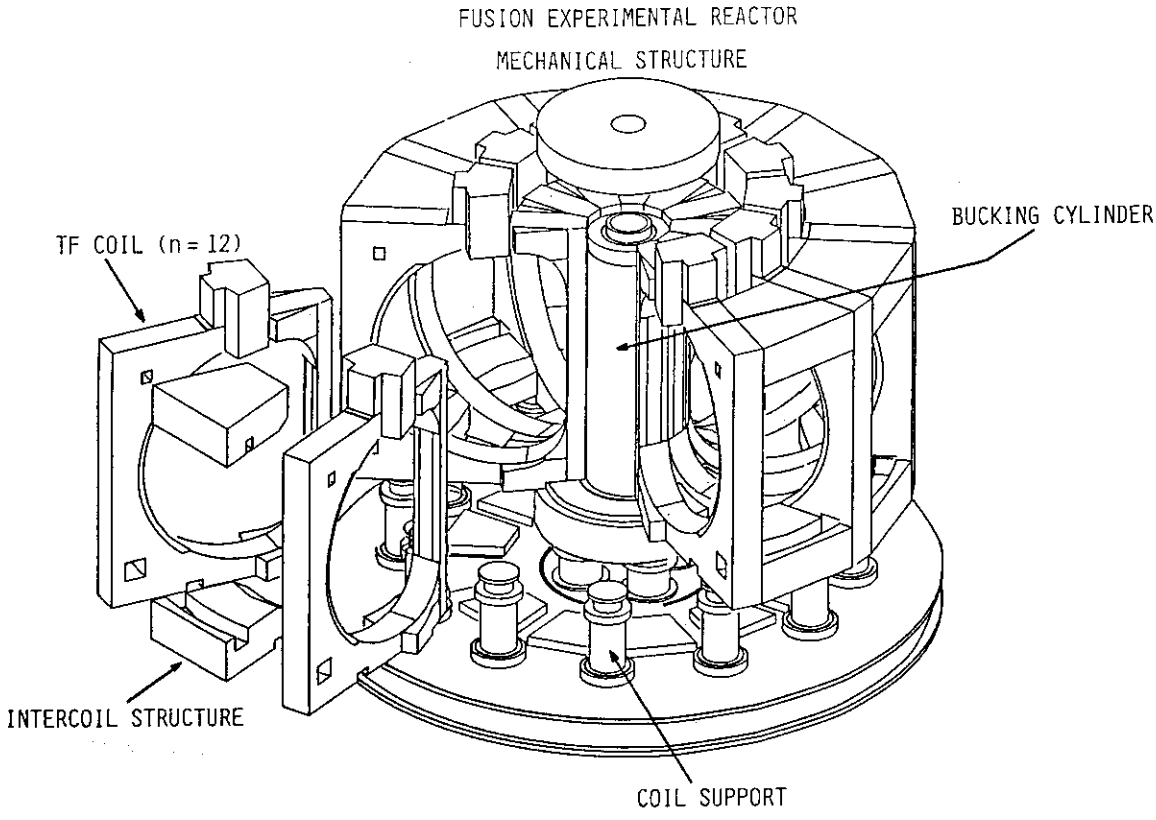

Fig. 1 Mechanical structure of the FER magnet system

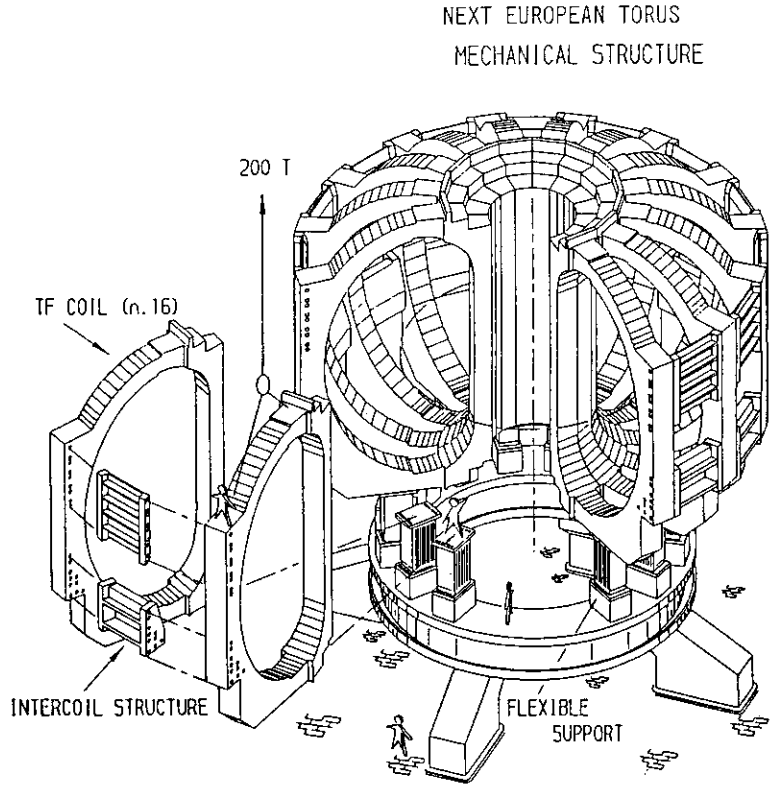

Fig. 2 Mechanical structure of the NET magnet system

TF COIL INNER LEG SECTIONS AT MID-PLANE

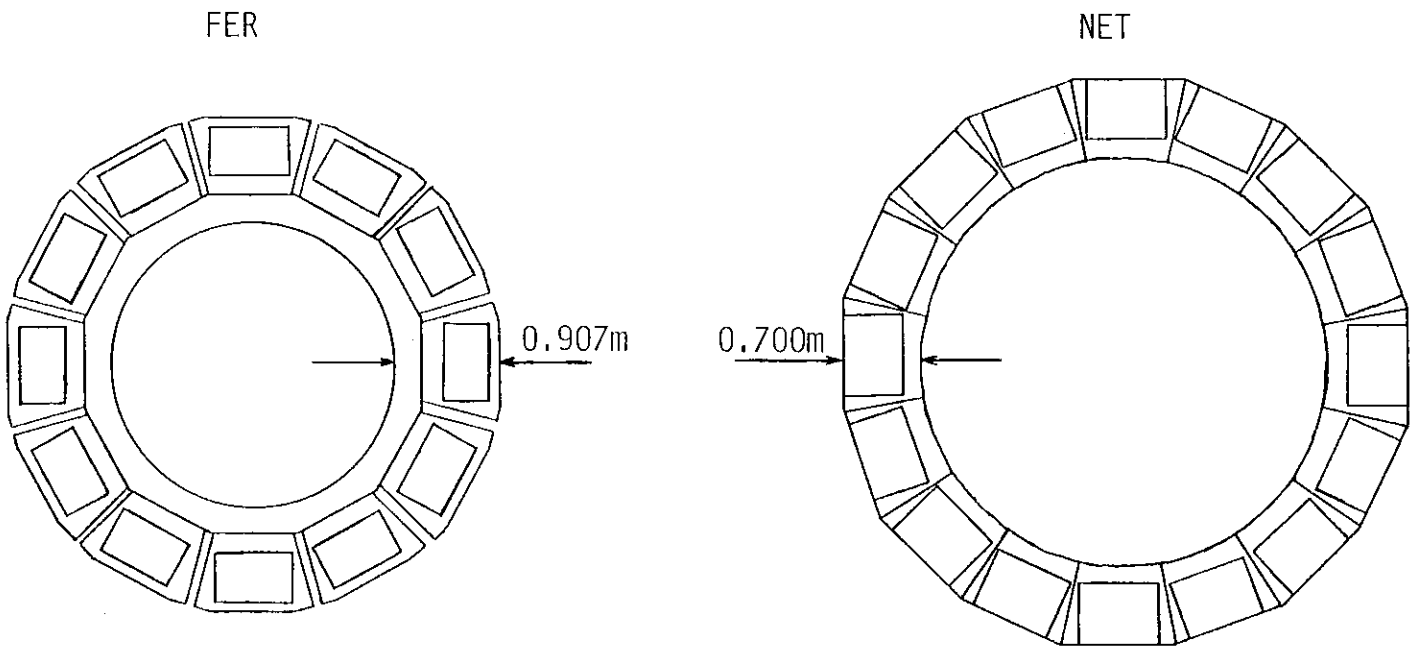

J_0 : Overall Current Density

Fig. 3 Sectional view of the TF coil inner legs at mid-plane

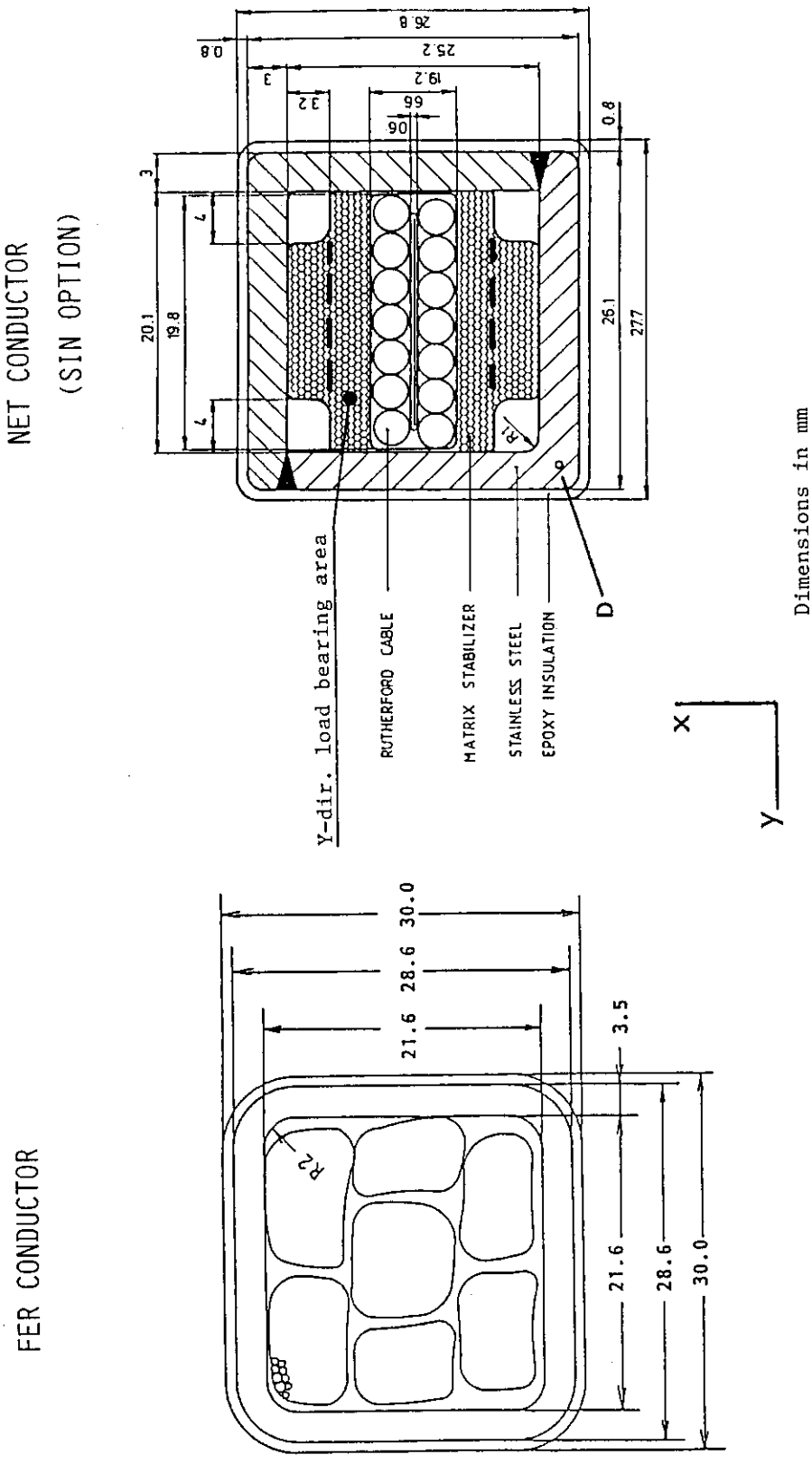

Fig. 4 TF coil conductor cross-sections

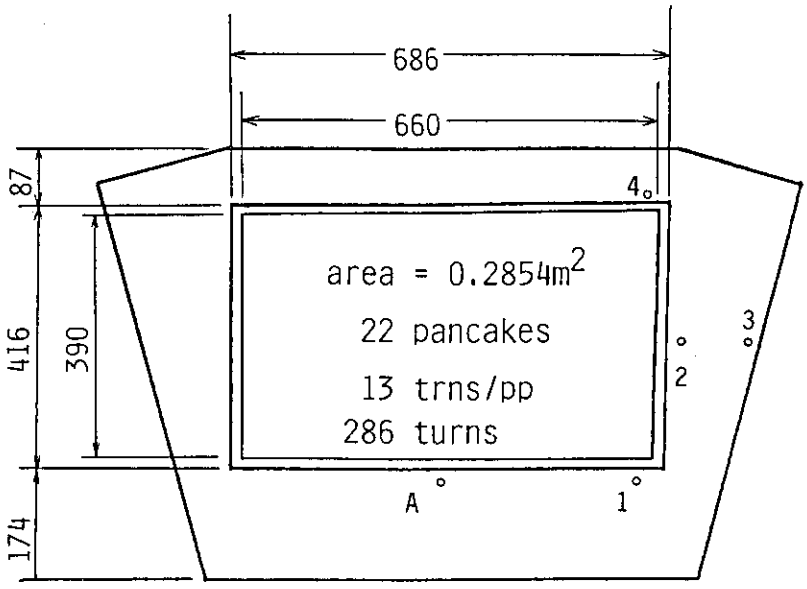

FER

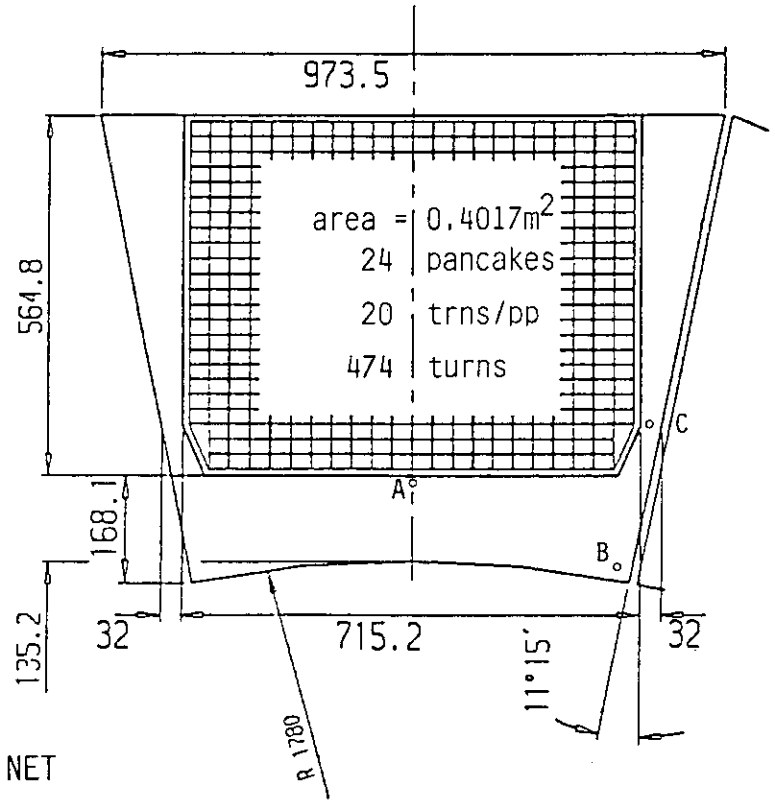

NET

Fig. 5 TF coil inner leg cross sections

NET uses wedging of the TF coils to react the centering force, F_x. The coils become compressed in the toroidal direction.

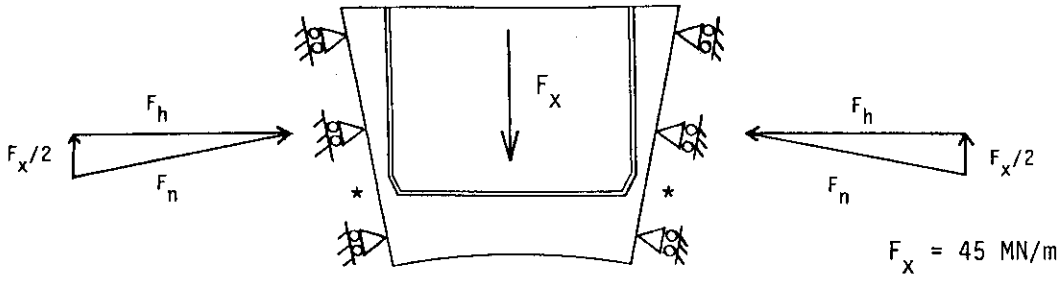

* Toroidal strain along the coil boundary is constant

MODEL:

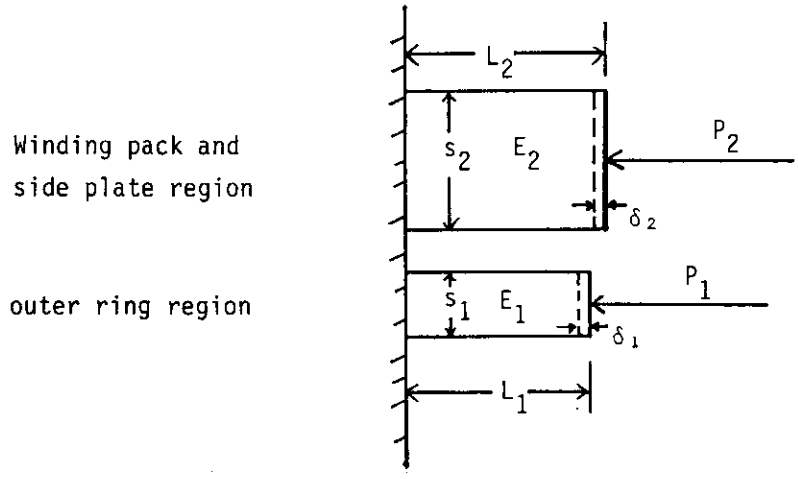

Since $\delta_1/L_1 = \delta_2/L_2$, then $\frac{P_1}{s_1E_1} = \frac{P_2}{s_2E_2}$. Also,

$P_1 + P_2 = F_h = 114$ MN/m. Hence,

$P_1 = 0.46 * F_h = 52$ MN/m, $P_2 = 0.54 * F_h = 62$ MN/m

Fig. 6 Static force diagram of the NET inner leg

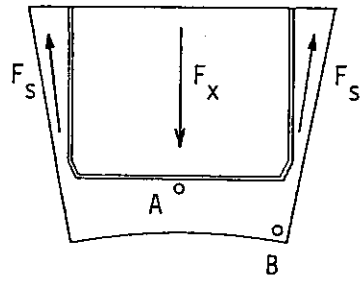

Side plates pull on vault and cause bending of the vault. Assuming NO friction between the winding pack and the side plates: $F_s = \frac{\sigma_2 s_2 \pi}{16} = \frac{P2\pi}{16}$

MODEL: cylinder of outer rings with discrete loads F_s

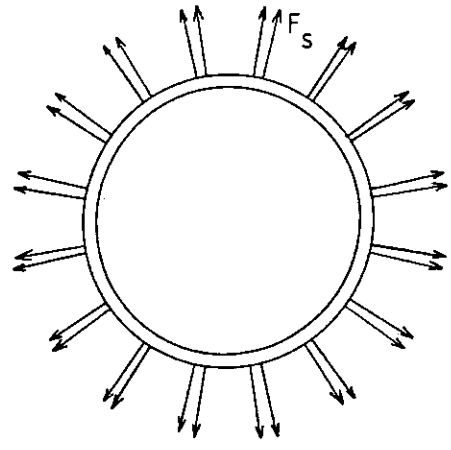

Friction between the winding pack and side plates reduces F_s by $F_f = k_f P_2$

Fig. 7 Bending of NET's outer ring

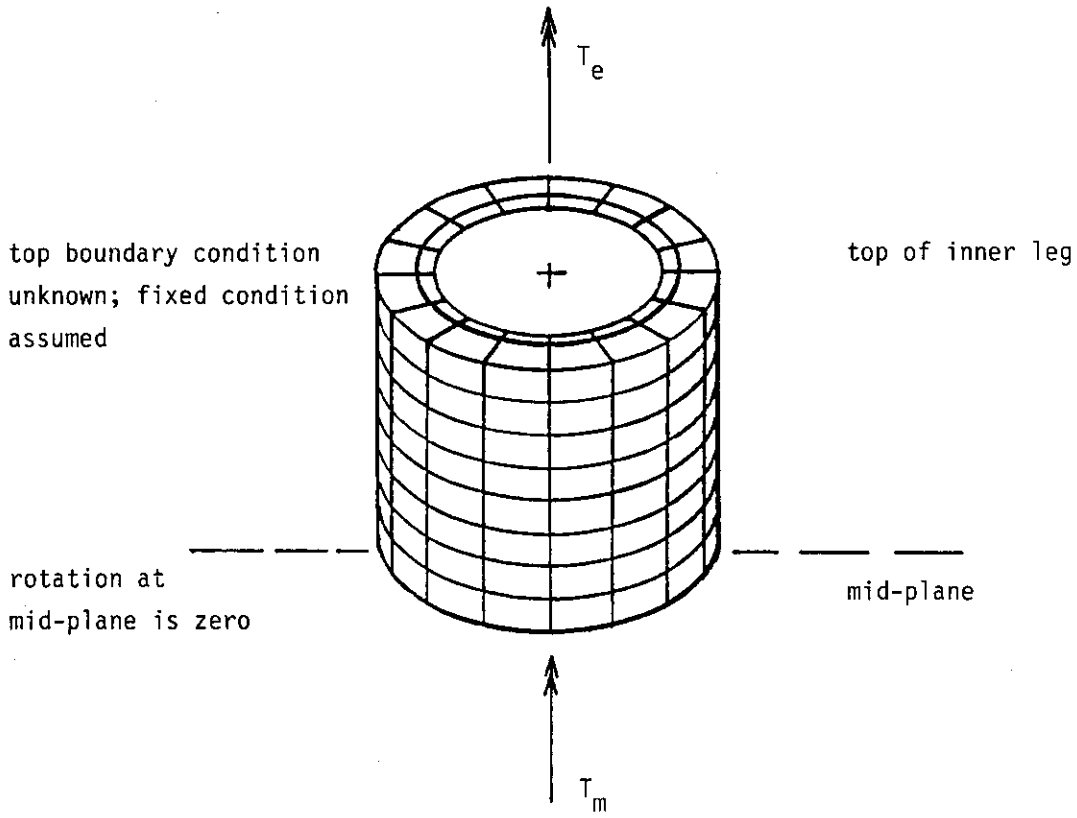

Two concentric cylinders are used to model the straight sections of the inner legs twisting from the distributed out-of-plane force. The inside cylinder models the outer rings; the outside cylinder models the winding packs and side plates. Both cylinders must rotate the same amount for compatibility. An energy method is used.

Fig. 8 NET's inner legs modelled as composite cylinder under torsion from out-of-plane forces

Appendix A Analyses Methods Additional Notes

TABLE A1

NET INNER LEG OUT-OF-PLANE FORCES & TORSION ESTIMATION
FORCES DURING END OF BURN
(from ref. 5)

segment I	1 z-position <m>	2 F_{ave} <MN/m>	3 T_{seg} <MN-m>	4 sumT(I) <MN-m>
END	3.555			
1		11.1	174.2	174.2
	3.110			
2		13.7	215.0	389.3
	2.666			
3		15.2	238.6	627.8
	2.222			
4		16.2	254.2	882.1
	1.777			
5		15.3	240.2	1122.2
	1.333			
6		11.9	186.7	1309.0
	0.889			
7		7.6	119.4	1428.3
	0.444			
8		3.6	56.5	1484.8
MID-PLANE	0.000			
			TOTAL =	7417.7

$T_{seg} = F_{ave} * deltaZ * R_{wp} * NTFC$, where:

deltaZ = 3.555/8 = 0.444 m

R_{wp} = 2.2 m

NTFC = 16

$sumT(I) = T_{seg}(1) + T_{seg}(2) + \ldots + T_{seg}(I)$

T_e = TOTAL/8 = 927.2 MN-m

ESTIMATION OF SHEAR MODULUS OF OUTSIDE CYLINDER

Using the values from ref. 1 for the winding pack:

$$E_{wp} = 77 \text{ GPa}, \quad \nu_{wp} = 0.33, \quad \text{then}$$

$$G_{wp} = \frac{E_{wp}}{2(1+\nu)} = 29 \text{ GPa}$$

Refer to Figs. 4 and 5. Use $G_{ins/ep} = 8$ GPa, and $G_{steel} = 80$ GPa.

G_{wp} is decreased because of ground insulation in X direction:

$$\frac{20(.0268)(29) + (.5648 - 20(.0268))(8)}{.5648} = 28 \text{ GPa}$$

The mean side plate thickness tsp = 0.0795 is in series with the winding pack:

$$\frac{24(.0277)}{28} + \frac{(.7152 - 24(.0277))}{8} + \frac{2(.0795)}{80} = \frac{.7152 + 2(.0795)}{G_o}$$

gives $G_o = 27$ GPa.

Appendix B Subroutine Output for FER ACS-M and NET DN

B1. Bucked TF Coil (FER ACS-M)

```
**************************************************
***   STRESS ANALYSIS OF TFC CASE AT INNER LEG   ***
***       FOR INITIAL TFC CASE DESIGN            ***
**************************************************

  TOROIDAL FIELD COIL STRESS ANALYSIS, STAGE 1
  ESTIMATED STRESSES FROM IN-PLANE FORCES FOR:  BUCKED TF COIL (LIKE FER)

  MATERIAL OF COIL CASE          :     SS304N       MATERIAL OF CONDUIT            :     SS304N
  WINDING THICKNESS W/O INSUL.   :     0.386<M>     WINDING WIDTH W/OUT INSULATOR  :     0.654<M>
  OUTER RING THICKNESS           :     0.189<M>     INNER RING THICKNESS           :     0.100<M>
  SIDE PLATE THICKNESS           :     0.176<M>     INSULATOR THICKNESS            :     0.0  <M>

DESIGN CONSTRAINTS FOR TFC CASE    :
  YIELD STRENGTH OF COIL CASE          :  7.652E+02<MPA>
  TENSILE STRENGTH OF COIL CASE        :  1.648E+03<MPA>
  ALLOWABLE STRESS INTENSITY FOR VON-MISES STRESS OF COIL CASE  : 510.E+00<MPA>
  SAFETY FACTORS ARE AS :    SF1= 1.00;  SF2= 1.00;  SF3= 1.00

  INPLANE CENTERING FORCE              :  4.311E+07<N/M>
  DISTRIBUTED LOAD BY CENTERING FORCE  :  6.596E+01<MPA>
  INPLANE VERTICAL FORCE               :  6.988E+07<N/M>

  MATERIAL OF BUCKING CYLINDER  :  SS304N
  BUCKING CYLINDER THICKNESS    :    0.230<M>
  YOUNG MODULUS                 : 206.E+00<GPA>
  POISSON RATIO                 : 0.2750

DESIGN CONSTRAINTS FOR BUCKING CYLINDER    :
  YIELD STRENGTH OF BUCKING CYLINDER    :  7.652E+02<MPA>
  TENSILE STRENGTH OF BUCKING CYLINDER  :  1.648E+03<MPA>
  ALLOWABLE STRESS INTENSITY FOR PRIMARY MEMBRANE STRESS OF BUCKING CYLINDER : 510.E+00<MPA>
  BUCKING CYLINDER SAFETY FACTORS ARE AS :   SF4= 1.00;  SFB= 4.00

  AVERAGE COMPRESSIVE STRESS OF BUCKING CYLINDER          : 358.E+00<MPA>
  ALLOWABLE COMPRESS. STRESS OF BUCKING CYLINDER  (SF4)   : 510.E+00<MPA>
  ALLOWABLE BUCKLING STRESS OF BUCKING CYLINDER   (SFB)   : 516.E+00<MPA>

 TOTAL COIL AREA =  0.6461,  COIL CASE AREA =  0.3940,   VERTICAL STRAIN =  7.11E-04

 INNER LEG STRESSES IN BUCKED CASE OUTER RING NEAR THE WINDING PACK:
   SIGMA X IN OUTER RING  : -66.E+00<MPA>
   SIGMA Y IN OUTER RING  :      0.0<MPA>
   SIGMA Z IN ALL STEEL   : 146.E+00<MPA>
   VON MISES STRESS       : 188.E+00<MPA>

 CONDUCTOR STRESSES:
 INNER LEG CONDUCTOR CONDUIT STRESSES NEAR THE OUTER RING:
   SIGMA X IN CONDUIT     :-261.E+00<MPA>
   SIGMA Y IN CONDUIT     :      0.0<MPA>
   SIGMA Z IN ALL STEEL   : 146.E+00<MPA>
   VON MISES STRESS       : 357.E+00<MPA>
```

```
*************************************************
***   STRESS ANALYSIS OF TFC CASE AT INNER LEG   ***
***       FOR INITIAL TFC CASE DESIGN            ***
*************************************************

  TOROIDAL FIELD COIL STRESS ANALYSIS, STAGE 2
  STRESSES ESTIMATED WITH OUT-OF-PLANE FORCES FOR:  BUCKED TF COIL (LIKE FER)

  ESTIMATED TORSIONAL SHEAR STRESSES IN TF INNER LEG FROM OUT OF PLANE FORCES:
  BUCKED/KEYED MAGNET--ALL TORSION CARRIED BY INNER RINGS


 RESULTS AT *****  IGNITION APPROACH *****
   SHEAR TYZ AT TOP END    :  26.E+00<MPA>
   SHEAR TYZ AT BOTTOM END:  66.E+00<MPA>
   SHEAR TYZ AT MIDPLANE   : -19.E+00<MPA>


 RESULTS AT *****  BEGINNING OF BURN *****
   SHEAR TYZ AT TOP END    :  18.E+00<MPA>
   SHEAR TYZ AT BOTTOM END:  56.E+00<MPA>
   SHEAR TYZ AT MIDPLANE   : -16.E+00<MPA>


 RESULTS AT *****  END OF BURN       *****
   SHEAR TYZ AT TOP END    :  42.E+00<MPA>
   SHEAR TYZ AT BOTTOM END:  74.E+00<MPA>
   SHEAR TYZ AT MIDPLANE   : -23.E+00<MPA>

 MAX TORQUE IN ALL INNER LEGS    :  2.103E+08<N-M>

 MAXIMUM SHEAR STRESS IN INNER RINGS :
   MAXIMUM TYZ             :  74.E+00<MPA>
   MAX OCCURS DURING       :  END OF BURN
   NEAR ZPOS               :    -3.06<M>

  APPROXIMATE MAX SHEAR STRESS IN SHEAR KEYS:
  MAX SHEAR IN SHEAR KEYS :  66.E+00<MPA>
  NEAR ZPOS               :    -3.06<M>

 MAX LOCAL OVERTURNING FORCE  :  1.33E+07<N/M>
 MAX LOCAL OVERTURNG PRESSURE :  3.45E+07<PA>
 OCCURS NEAR Z-POSITION       : -3.06E+00<M>
 DURING                       :   END OF BURN

 LOCAL STRESSES DUE TO MAXIXMUM OUT-OF-PLANE FORCE :
   SIG32 IN OUTER RING     : 399.E-01<MPA>
   S3CAN2 IN INNER RING    : 987.E-01<MPA>
   S3CAN3 IN INNER RING    : 151.E+00<MPA>

 PRINCIPAL STRESS DUE TO MAX O-O-P FORCE AND SHEAR THERE :
   SIGP1 IN INNER RING     : 139.E+00<MPA>

 PRINCIPAL STRESS DUE TO MAX TORQUE AND LOCAL O-O-P FORCE THERE:
   SIGP2 =  139.E+00<MPA>

 VON-MISES ALLOWABLE STRESS IS : 510.E+00<MPA>

 ESTIMATED VON-MISES STRESSES FROM IN-PLANE AND MAXIMUM OUT-OF-PLANE LOCAL STRESSES :
 MAX AT ZPOS = -3.06<M> ; DURING   END OF BURN
   OUTER RING NEAR WINDING PACK CORNER, SVM4 : 131.E+00<MPA>
   MID SIDE PLATE NEXT TO WINDING PACK, SVM5 : 260.E+00<MPA>



   MID SIDE PLATE NEAR CASE OUTER EDGE, SVM6 : 149.E+00<MPA>

 VON-MISES FROM IN-PLANE, MAXIMUM O-O-P LOCAL, AND TORSIONAL SHEAR :
 MAX AT ZPOS = -3.06<M> ; DURING   END OF BURN
   IN INNER RING NEAR CASE OUTER EDGE,  SVM6 : 183.E+00<MPA>

 VON-MISES FROM IN-PLANE, MAXIMUM TORSIONAL SHEAR, AND O-O-P LOCAL STRESSES :
 MAX AT ZPOS = -3.06<M> ; DURING   END OF BURN
   IN INNER RING NEAR WIND/PACK CORNER, SVM7 : 183.E+00<MPA>

 EST. BENDING STRESS OF INNER LEG UNDER WORST CASE
 ASSUMPTION OF FAILED SHEAR KEYS OR WEDGE FRICTION :
   CASE BENDING STRESS     : 640.E-01<MPA>
   MAX OCCURS DURING       :  IGNITION APPROACH
   NEAR ZPOS               :    -3.06<M>
```

B2. Wedged TF Coil (NET DN)

```
*****************************************************
***   STRESS ANALYSIS OF TFC CASE AT INNER LEG    ***
***       FOR INITIAL TFC CASE DESIGN             ***
*****************************************************

  TOROIDAL FIELD COIL STRESS ANALYSIS, STAGE 1
  ESTIMATED STRESSES FROM IN-PLANE FORCES FOR:  WEDGED TF COIL (LIKE NET)

  MATERIAL OF COIL CASE          :     SS304N       MATERIAL OF CONDUIT            :     SS304N
  WINDING THICKNESS W/O INSUL.   :     0.557<M>     WINDING WIDTH W/OUT INSULATOR  :     0.611<M>
  OUTER RING THICKNESS           :     0.135<M>     INNER RING THICKNESS           :     0.0  <M>
  SIDE PLATE THICKNESS           :     0.116<M>     INSULATOR THICKNESS            :     0.015<M>

DESIGN CONSTRAINTS FOR TFC CASE    :
  YIELD STRENGTH OF COIL CASE          :  7.652E+02<MPA>
  TENSILE STRENGTH OF COIL CASE        :  1.648E+03<MPA>
  ALLOWABLE STRESS INTENSITY FOR VON-MISES STRESS OF COIL CASE  : 510.E+00<MPA>
  SAFETY FACTORS ARE AS :    SF1= 1.00;  SF2= 1.00;  SF3= 1.00

  INPLANE CENTERING FORCE              :  4.213E+07<N/M>
  DISTRIBUTED LOAD BY CENTERING FORCE  :  6.891E+01<MPA>
  INPLANE VERTICAL FORCE               :  7.252E+07<N/M>

 TOTAL COIL AREA =  0.6195,  COIL CASE AREA =  0.2428,   VERTICAL STRAIN =  8.23E-04

 INWARD RADIAL DISPACEMENT OF WEDGED COIL  :   2.31<MM>

 COEFFICIENT OF FRICTION BETWEEN WINDING PACK AND SIDE PLATE IS :  0.0

 INNER LEG STRESSES IN MIDDLE OF WEDGED CASE OUTER RING NEAR THE WINDING PACK:
   SIGMA X IN OUTER RING  : -69.E+00<MPA>
   SIGMA Y IN OUTER RING  :-293.E+00<MPA>
   SIGMA Y BENDING IN OR  :-268.E+00<MPA>
   SIGMA Z IN ALL STEEL   : 170.E+00<MPA>
   VON MISES STRESS       : 645.E+00<MPA>

 INNER LEG STRESSES IN WEDGED CASE OUTER RING NEAR THE CASE CORNER:
   SIGMA X IN OUTER RING  :      0.0<MPA>
   SIGMA Y IN OUTER RING  :-229.E+00<MPA>
   SIGMA Y BENDING IN OR  :-220.E+00<MPA>
   SIGMA Z IN ALL STEEL   : 170.E+00<MPA>
   VON MISES STRESS       : 554.E+00<MPA>

 INNER LEG STRESSES IN WEDGED SIDE PLATE AT NARROWEST SECTION:
   SIGMA X IN SIDE PLATE  : 169.E+00<MPA>
   SIGMA Y IN SIDE PLATE  :-115.E+00<MPA>
   SIGMA Z IN ALL STEEL   : 170.E+00<MPA>
   VON MISES STRESS       : 284.E+00<MPA>

 CONDUCTOR STRESSES:

 APPROXIMATE MAX STRESSES IN CONDUCTOR CONDUIT AT MID-PLANE:
   SIGMA X IN CONDUIT     :-325.E+00<MPA>
   SIGMA Y IN CONDUIT     :-261.E+00<MPA>
   SIGMA Z IN CONDUIT     : 170.E+00<MPA>
   VON MISES STRESS       : 466.E+00<MPA>

 APPROXIATE MAX STRESSES IN CONDUCTOR STABILIZER NEAR THE OUTER RING:
   SIGMA X IN STABILIZER  :      0.0<MPA>
   SIGMA Y IN STABILIZER  :-174.E+00<MPA>
   SIGMA Z IN STABILIZER  : 823.E-01<MPA>
   VON MISES STRESS       : 227.E+00<MPA>



****** VON-MISES CHECKS =  2

++++++++++++++++++++++++++++++++++++++++++++++++++++
   RADIAL BUILD AND PLASMA CALCULATION SHOULD BE
  MODIFIED DUE TO OVERSTRESS FROM IN-PLANE FORCES
    ***VON-MISES CRITERIA HAS BEEN EXCEEDED***
++++++++++++++++++++++++++++++++++++++++++++++++++++
```

```
**************************************************
***   STRESS ANALYSIS OF TFC CASE AT INNER LEG   ***
***       FOR INITIAL TFC CASE DESIGN            ***
**************************************************

  TOROIDAL FIELD COIL STRESS ANALYSIS, STAGE 2
  STRESSES ESTIMATED WITH OUT-OF-PLANE FORCES FOR:  WEDGED TF COIL (LIKE NET)

  ESTIMATED TORSIONAL SHEAR STRESSES IN TF INNER LEG FROM OUT OF PLANE FORCES:
  WEDGED MEGNET--TORSION SHARED BETWEEN OUTER RINGS, WP/SP AND INNER RINGS


 RESULTS AT *****  IGNITION APPROACH *****

 SHEAR STRESSES IN OUTER RINGS :
   SHEAR TYZT1 AT TOP END    :  90.E+00<MPA>
   SHEAR TYZB1 AT BOTTOM END:  87.E+00<MPA>
   SHEAR TYZMD1 AT MIDPLANE : -33.E+00<MPA>

 SHEAR STRESSES IN WINDING-PACK/SIDE-PLATES  :
   SHEAR TYZT2 AT TOP END    :  52.E+00<MPA>
   SHEAR TYZB2 AT BOTTOM END:  51.E+00<MPA>
   SHEAR TYZMD2 AT MIDPLANE : -19.E+00<MPA>


 RESULTS AT *****  BEGINNING OF BURN *****

 SHEAR STRESSES IN OUTER RINGS :
   SHEAR TYZT1 AT TOP END    :  65.E+00<MPA>
   SHEAR TYZB1 AT BOTTOM END:  62.E+00<MPA>
   SHEAR TYZMD1 AT MIDPLANE : -31.E+00<MPA>

 SHEAR STRESSES IN WINDING-PACK/SIDE-PLATES  :
   SHEAR TYZT2 AT TOP END    :  38.E+00<MPA>
   SHEAR TYZB2 AT BOTTOM END:  36.E+00<MPA>
   SHEAR TYZMD2 AT MIDPLANE : -18.E+00<MPA>


 RESULTS AT *****  END OF BURN       *****

 SHEAR STRESSES IN OUTER RINGS :
   SHEAR TYZT1 AT TOP END    :  65.E+00<MPA>
   SHEAR TYZB1 AT BOTTOM END:  63.E+00<MPA>
   SHEAR TYZMD1 AT MIDPLANE : -31.E+00<MPA>

 SHEAR STRESSES IN WINDING-PACK/SIDE-PLATES  :
   SHEAR TYZT2 AT TOP END    :  38.E+00<MPA>
   SHEAR TYZB2 AT BOTTOM END:  37.E+00<MPA>
   SHEAR TYZMD2 AT MIDPLANE : -18.E+00<MPA>

 MAXIMUM SHEAR STRESS IN INNER LEGS :
   MAX TYZ OUTER RINGS     :  90.E+00<MPA>
   MAX TYZ WIND-P/S-PLATES:  52.E+00<MPA>
   MAX TYZ INNER RINGS     :   0.E+00<MPA>
   MAX OCCURS DURING       :  IGNITION APPROACH
   NEAR ZPOS               :     4.12<M>

 MAX TORQUE IN ALL INNER LEGS    :  1.202E+09<N-M>

  VON-MISES ALLOWABLE STRESS IS : 510.E+00<MPA>

 ESTIMATED VON-MISES STRESSES FROM IN-PLANE AND MAXIMUM TORSIONAL SHEAR STRESSES :



 MAX AT ZPOS =  4.12<M> ; DURING   IGNITION APPROACH
   MID OUTER RING NEAR WINDING PACK,     SVM4 : 680.E+00<MPA>
   OUTER RING NEAR CASE CORNER,          SVM5 : 576.E+00<MPA>
   NARROW SECTION OF SIDE PLATE ,        SVM6 : 298.E+00<MPA>

 EST. BENDING STRESS OF INNER LEG UNDER WORST CASE
 ASSUMPTION OF FAILED SHEAR KEYS OR WEDGE FRICTION :
   CASE BENDING STRESS     : 388.E+00<MPA>
   MAX OCCURS DURING       :  IGNITION APPROACH
   NEAR ZPOS               :    -4.12<M>

****** VON MISES CHECKS =  2

++++++++++++++++++++++++++++++++++++++++++++++++++
   RADIAL BUILD AND PLASMA CALCULATION SHOULD BE
      MODIFIED DUE TO OVERSTRESS FROM COMBINED
         IN-PLANE AND OUT-OF-PLANE FORCES.
    ***VON-MISES CRITERIA HAS BEEN EXCEEDED***
++++++++++++++++++++++++++++++++++++++++++++++++++
```

Appendix C Subroutine Notes

STAGE 1 IN-PLANE SUBROUTINE NOTES:

1. Winding pack area INCLUDES the ground insulation. Old subroutine did not include the ground insulation thickness (TINS).

2. NEW data required as input:

FSS - for both bucked and wedged options, the area fraction of stainless steel conduit over the winding pack area as defined in 1.

FSTA - for wedged options only, the area fraction of stabilizing material over the wp area

FSC - wedged type, fraction of super conductor

YNGSTA - Young's modulus of stabilizer

YNGSCD - Young's modulus of superconductor

EWPY - both types input (but still used only wedged type); Equivalent Young's modulus of winding pack in Y direction (toroidal direction), including the ground insulation

EMODY2 - Wedged type, equivalent modulus of limitin load bearing section (Y-dir). See sect. 2.1 - eqn 3

FK - wedged type, assumed coefficient of friction between winding pack and side plates

2. NEW variables used INSIDE subroutine, change as appropriate:

SMB - Saftey factor for buckling allowable stress of bucking cylinder

3. Safety factor SF1 is applied for Von Mises allowable stress

4. Saftey factor SF4 is applied for toroidal allowable stress of bucking cylinder

STAGE 2 OUT-OF-PLANE SUBROUTINE NOTES:

1. NEW variables used INSIDE subroutine, change as appropriate:

   FKEY - Factor to multiply times inner ring thickness to give X direction (radial) thickness of shear keys

   POIS2 - Equivalent poisson's ratio of winding pack - side plate region to give approximate shear modulus based on EY value calc'd in stage 1. see sect 2.2 Part II.

   SCYC - Cyclic allowable stress- is changed by safety factor SF2

2. Out-of-plane routine loops over operation time phases: Ignition approach; Beginning of burn; End of burn. Forces on straight part of inner leg are used only-- they come from PFONTF subrouitine.

   For each time phase, the max force (in N/m) is found, to be used for max local stresses for bucked type. These are at the ends of the segments of the inner leg (10 segments).

   Average values (at middle of each inner leg segment) are found and stored.

   Also, the the force (N) generated in each of the 10 segments of the inner leg are found.

   Sums and accumulated sums of these forces are made as described in sect. 3.1 and appendix A. SUM1 and SUM2 are only for worst case bending of inner leg estimate--not for torsion solution.

   Z position of max torque location (and max moment) is not so precise because of discretizing of inner leg.

   Shear stress estimates based on MEAN radius to respective "cylinders", considering that uncertainty in estimate makes using the MAX radius unfairly pessimistic.

3. The stage 2 subroutine includes a function for evaluating PRINCIPAL stress for cyclic criteria; A function for Von Mises stress was added to TRESCODE independently.

4. The worst case bending stress estimation may be the crudest estimate included. It is also based on an energy method of a discretized beam with fixed ends and a distributed load. The distributed load is approximated by loads acting at the middle of each segment. The chosen redundant reactions are the top moment and transverse force. Moment equations are written as a function of the point loads, top moment and force, distance from the top of the inner leg. Integrals written (2) for the change in bending energy with respect to the top moment and top force are simplified in terms of the unknowns top moment and top force, the applied loads (which make SUM1 and SUM2), and the length of the straight inner leg. With top moment and top force known, the moment at each position can be found. Then the maximum must be found.

The area modulus of the case and winding pack are evaluated. The assumption is used that the bending strain is equal between the case and winding pack, so the case reacts a fraction of the moment at any Z position (eqn 25). The bending stress in the case is obtained then.